The Thesis Committee for David John Szafron Certifies that this is the approved version of the following thesis:

Development of an image based technique for assessment of colorectal epithelial integrity and function in an ovine model

Committee:

_____

Massoud Motamedi, PhD, Mentor

_____

Gracie Vargas, PhD

_____

Karl Anderson, MD

_____

Dean, Graduate School

Development of an image based technique for assessment of colorectal epithelial integrity and function in an ovine model

by

David John Szafron, BS

Thesis

Presented to the Faculty of the Graduate School of

The University of Texas Medical Branch

in Partial Fulfillment

of the Requirements

for the Degree of

Masters of Science

The University of Texas Medical Branch
July 2016

Dedication

To my fiancé Vibha and my loving family.

Acknowledgements

Development of an image based technique for assessment of colorectal epithelial integrity and function in an ovine model

Publication No._____

David John Szafron, MS

The University of Texas Medical Branch, 2016

Supervisor: Massoud Motamedi

Damage to the intestinal epithelium can cause alterations in barrier permeability and may lead to an inflammatory state. This alteration in permeability may lead to or be a consequence of several disease states. Confocal endomicroscopy (CE) is an emerging technology capable of assessing mucosal permeability and structure during endoscopy. Chapter 2 assesses the alteration in rectal permeability in an ovine model induced by introduction of the microbicidal agent benzalkonium chloride (BZK). The study utilizes CE to demonstrate that BZK causes a significant increase in permeability on a 3-point visual grading scale as assessed by three graders between untreated (1.19 ± 0.53) and BZK treated (2.55 ± 0.75) tissues. Increased permeability may result in increased susceptibility to infections such as HIV. Chapter 3 expands on the permeability measures performed in Chapter 2 by introducing a novel quantitative grading technique. This method utilizes the grey level co-occurrence matrix (GLCM) texture analysis technique to compute the correlation statistic for each image. ROC analysis produces an ideal cut-off point for determining an increase in permeability with a resultant sensitivity and specificity of 95.5%. Quantitative permeability measures expand the applications of CE permeability assessment and strengthen its use in real time assessment of functional

permeability in the clinic. Chapter 4 applies this newly developed technique to an ovine model in which estrogen and progesterone levels are altered. Past studies indicate that estrogen strengthens tight junctions and reduces permeability of the gut when present. This study finds that sheep that have been hormonally suppressed with depot medroxyprogesterone have a high permeability with 50% of sites showing increased permeability via the GLCM method developed in Chapter 3. Estrous phase normally cycling sheep have increased permeability in only 12.5% of sites. This study further finds other differences between hormonal states in the form of inflammation and epithelial gaps. The combination of quantitative permeability assessment with the structural information gathered by CE makes it an emerging technique that may expand our ability to diagnose and treat numerous gastrointestinal diseases during routine endoscopy.

TABLE OF CONTENTS

List of Tables

List of Figures

List of Abbreviations

AIDS	Acquired immunodeficiency syndrome
BZK	Benzalkonium chloride
CDC	Centers for disease control and prevention
CE	Confocal endomicroscopy
DPTA	Diethylenetriamine pentaacetate
EGD	Esophagogastroduodenoscopy
FL	Fluorescein
GLCM	Grey level co-occurrence matrix
H&E	Hematoxylin and eosin
HIV	Human immunodeficiency virus
IACUC	Institutional animal care and use committee
IBD	Inflammatory bowel disease
IBS	Irritable bowel syndrome
NIH	National institute of health
OCT	Optical coherence tomography
PBS	Phosphate buffered saline
ROC	Receiver operating characteristic
UC	Ulcerative colitis
UTMB	University of Texas Medical Branch

Chapter 1 Introduction

CONFOCAL ENDOMICROSCOPY

Gastrointestinal mucosal surfaces may be evaluated by a variety of means to examine characteristics such as structure and function. Detection of alterations in these characteristics aids in the diagnosis and determination of appropriate treatment for various diseases. For example, the gold standard for diagnosis of colorectal cancer is endoscopic evaluation accompanied by tissue biopsy specimens (1). The tissue biopsies are examined with the assistance of traditional staining such as H&E, or with more advanced and specific staining techniques such as immunohistochemistry (2). Qualitative grading is used to evaluate the histologic images. These traditional methods provide reliable means for assessing and diagnosing gastrointestinal diseases, but are invasive and do not provide real time diagnosis. In addition, there is a risk of selecting a biopsy site that does not provide sufficient tissue to provide a diagnosis. This situation necessitates repeated biopsy and can lengthen the diagnosis process.

Advances in imaging techniques have allowed for the development of optical biopsies instead of traditional tissue biopsy. Specifically, confocal microscopy of mucosal surfaces can provide real time images without the need for biopsy and subsequent lab analysis (3, 4). This process can be used in place of tissue biopsy or to help guide site selection to allow for a biopsy to be taken from areas of highest suspicion for pathology. Additionally, the confocal microscope is able to scan below the surface to view structures at depths of up to 70 microns (5, 6). Confocal microscopy relies on the use of a pinhole to eliminate out-of-focus light when imaging, allowing for optical

sectioning and reconstruction of images. The confocal microscope has been adapted to integrate into flexible endoscopes, allowing real time confocal imaging during endoscopic procedures such as EGD and colonoscopy. The Pentax EC3870K is an endoscope with an integrated confocal endomicroscope with a rigid portion of only 5 cm (6).

This imaging modality provides an alternative to traditional methods such as tissue biopsy during colonoscopy in the case of colorectal cancer diagnosis above. The use of contrast agents to enhance visibility of the imaged tissue has been used to delineate nuclei and other structures (7). Fluorescein and acriflavine dyes represent the most commonly used options. Fluorescein is often administered intravenously and allows for imaging of vascular structures and can be used to determine functional permeability. On the other hand, acriflavine is applied locally and stains the cell nuclei, allowing individual cells to be seen more easily (7).

Along with the correct contrast agent, confocal endomicroscopy has been shown to accurately diagnose intraepithelial neoplasia and colorectal cancer in humans (1). Kiesslich et al examine confocal images graded on cellular and vascular changes in comparison to traditional histology. The grading system provides a basis for grading of colonic CE images similar to systems used in traditional H&E image analysis. In this study, both acriflavine and fluorescein dyes were utilized. Ultimately, fluorescein is recommended for screening due to its ability to delineate structures below the mucosal surface and its ability to visualize vasculature (1).

In addition to screening for colorectal cancer, CE has also gained use as a screening method for other cancers and has been used during operative procedures.

Barret's esophagus, a precursor metaplastic lesion to esophageal cancer, results in

transformation of normal stratified squamous epithelium of the esophagus to columnar

epithelium (3, 8). CE is able to image esophageal epithelium during EGD of patients who

are at risk of Barret's esophagus. CE is also used during operative procedures as an

alternative to histological analysis by frozen sectioning. For example, confocal

microscopy can assess tumor borders during resection surgery for cancers. In

neurosurgical procedures for the resection of primary brain carcinomas such as

glioblastoma and meningioma, confocal microscopy can supplement fast

histopathological guidance for decision making in determining margins (9). The use of

CE and confocal microscopy to replace or augment histopathology may lead to hastened

and improved diagnoses in clinical settings. Real-time imaging can also guide biopsy site

selection in cases when histopathology is required.

      While CE has been shown to be useful in screening for cancer, it also has

potential applications in other situations in which mucosal damage occurs. The disease

course of inflammatory bowel disease is variable, but it is often characterized by

intermittent flares of severe disease along with periods of mild disease (10, 11). Rapid

identification of flares is important to guide the treatment of disease. CE has been shown

to allow the prediction of relapse of IBD. In addition to evaluation of IBD, Kiesslich et al

also outline a grading system to evaluate confocal images for damage with the assistance

of intravenous fluorescein dye (10). This grading system can be modified and applied to

other inflammatory conditions and situations in which confocal imaging is used.

IRRITABLE BOWEL SYNDROME

Irritable bowel syndrome (IBS) is a chronic gastrointestinal disease characterized by abdominal pain with diarrhea or constipation. IBS represents a significant disease burden on many people around the world, with the prevalence increasing in recent years. In particular, studies have shown that IBS has a female predominance of around 4:1 over males (12). Additional risk factors for the disease include age in the 2nd or 3rd decade of life, comorbid chronic pain syndromes such as fibromyalgia, physical and emotional stress, and alcohol consumption (13). Clinically, IBS is defined by the Rome III criteria as abdominal discomfort along with 2 of 3 of the following symptoms: relief of pain with defecation, change in frequency of stool, or change in consistency of stool. These changes must persist for at least 3 months to be considered as irritable bowel syndrome (14). Patients often are described as having either diarrhea or constipation dominant IBS, but usually have symptoms of both. There are no specific tests to diagnose IBS as the pathogenesis of the disease remains unknown (15).

The pathogenesis of IBS is hypothesized to be a consequence of an increased permeability in the gut mucosa which leads to increased uptake of potential toxins from the gut lumen. Increased colonic permeability has been demonstrated in a portion of humans with a diagnosis of IBS as measured by colonic biopsies (16). A chronic inflammatory response is thought to develop due to this increased permeability and patients develop IBS. The supernatant from the IBS patient's colon results in an increase in permeability of healthy cells (16). These findings suggest that permeability and gut flora both have a role in the pathogenesis of IBS. However, there is also a subset of IBS patients that do not have altered gut permeability. The lactulose/mannitol test, often

referred to as the "leaky gut test," shows that only half of patients with IBS have increased permeability with this test (17). The lactulose mannitol test is performed by dissolving lactulose and mannitol in water given orally as a bolus administration. Serum or urine is collected every 2 hours after bolus administration (18). The serum or urine is tested for the absolute value and ratio of lactulose:mannitol. Lactulose level represents paracellular absorption and mannitol represents transcellular absorption. An increased ratio indicates that paracellular permeability is increased. A ratio of 0.07 is used as a standard cutoff to determine if paracellular transport is occurring (17). This test is much less expensive and less invasive than obtaining a colonic biopsy as in Piche et al. It uses the differential absorption of the sugars lactulose and mannitol through the paracellular and transcellular path as measured in blood or urine to determine gut permeability. However, the lactulose/mannitol test does not give a localized measure of permeability.

THE ROLE OF ESTROGEN IN IBS AND PERMEABILITY

The higher prevalence of IBS in females suggests that estrogen may play a role in mucosal integrity and acts throughout the gut on Estrogen Receptor β (19). A recent study in a murine model demonstrated that giving estrogen actually increases the expression of proteins used to create the tight junctions between mucosal cells such as occludin. This increased protein expression results in lower levels of gut permeability (20). Another study has shown that soy based food products that are developed to be high in estrogen content can similarly decrease the gut permeability and may be a potential treatment for patients with IBS (21, 22). However, the low estrogen state in menopause actually leads to decreased symptoms in patients with IBS instead of an increase as would be expected (12). Estrogen replacement in menopause can lead to exacerbation of

symptoms, but oral contraceptive use in pre-menopausal females can be protective (12, 23).

Despite the progress that has been made in characterizing the pathogenesis of IBS, there is still a need for a more complete model. Changes in permeability and the influence of hormones such as estrogen can only partially describe the pathogenesis of IBS. The reality is that IBS is likely a multifaceted disease that may have several different subtypes with similar but distinct mechanisms. The main challenges in the study of IBS have been the lack of a widely accepted animal model for the disease and the lack of a definitive diagnostic test.

HIV AND AIDS

HIV is a global epidemic, with more than 44,000 new cases in the United States per year, and many more around the world (24, 25). HIV treatments have evolved to better combat this infection, but prevention still represents a realistic and cost effective approach in the fight against HIV and AIDS. Mucosal surfaces provide a physical and chemical barrier to transmission of HIV and other infections. The rectal mucosal surface is particularly vulnerable to HIV infection and maintenance of this mucosal surface is essential to protecting against transmission of HIV and other pathogens (4, 26). Disruption of the rectal mucosal may occur due to multiple causes: physical means such as intercourse, chemical means such as lubricants or spermicides, or inflammatory conditions such as irritable bowel syndrome (25, 27-29).

Spermicides, microbicides, and lubricating gels have recently caused concern for an increased risk of transmission of HIV and other pathogens (30). They can result in destruction of the upper layers of the mucosal epithelium and increased mucosal

permeability. The gut mucosa has only a single layer of columnar epithelial cells above the lamina propria to protect from incursion of toxins and pathogens. Maintaining this layer is vital to preventing infection. These gels have been shown to denude and damage the epithelium. In particular, the spermicidal gel nonoxynyl-9 has been shown to increase susceptibility to infection by HIV and other sexually transmitted infections (31-35). Other microbicidal gels and lubricants likely cause similar results (36, 37).

It is critical to develop models to better test products such as microbicidal gels and lubricants to ensure the safety of users. *In vitro* models to test microbicidal gels such as nonoxynyl-9 and benzalkonium chloride are necessary. CE has evolved as a method to evaluate structural changes in real time after application of these agents. In addition to alterations in structure, perturbation of mucosal permeability may also be evaluated with the use of CE and an appropriate contrast agent.

AIMS OF STUDY

This study aims to characterize the permeability of gut mucosa, as well as examine the mucosa for microstructural changes using confocal endomicroscopy. Confocal endomicroscopy allows real-time imaging at a subcellular level during endoscopic procedures. Intravenously administered fluorescein dye can be used to assess paracellular permeability in real time. Locally applied acriflavine dye can enhance visualization of subcellular structures such as nuclei. A female sheep model is utilized due to similarity with human anatomy and physiology and to confirm findings from murine models. An ovine model is ideal due to cost effectiveness and size of animal. Murine models are not sufficiently large to allow assessment of confocal endomicroscopes that are sized for humans.

The role of estrogen in altering gut permeability may partially explain irritable bowel syndrome, but further study is needed. Past studies have shown that estrogen alters tight junction expression in a murine model. The next step is to test this in a large animal model with additional techniques to examine microstructure. Confocal endomicroscopy represents an ideal method to assess the hypothesized alterations in permeability due to estrogen. In addition, other observable changes in structure and function may be identified by confocal endomicroscopy at varying estrogen levels.

Aim 1 – Assess CE as a method for evaluating rectal mucosal structural and functional changes due to treatment with microbicides, with application for HIV prevention.

Aim 2 – Develop an image analysis algorithm to quantitatively evaluate rectal permeability by CE, with the goal to confirm findings in previous studies and use the algorithm in future studies.

Aim 3 – Extend the CE method and algorithm developed to assess the permeability and microstructure of the gut at varying estrogen levels, with the goal of better characterizing the effects of estrogen on diseases such as irritable bowel syndrome and inflammatory bowel disease.

Chapter 2 The Use of Confocal Endomicroscopy in a BZK Damage Model

SUMMARY

Confocal endomicroscopy was utilized to evaluate rectal mucosal barrier function to provide *in vivo* structural and functional barrier assessment. This was done following topical application of the microbicide BZK. The topical fluorescent probe acriflavine was utilized to provide subcellular resolution along with intravenously administered fluorescein dye to assess loss of barrier function and to assess functional permeability. A 3 point endoscopic grading system based on cellular integrity and leaking of fluorescein dye was utilized to assess damage. Biopsies were taken at the time of imaging for use in comparing the histopathology results with the endoscopic images.

370 images from six sheep were evaluated. These images were randomized into 100 images to be used as a training image set and 270 images to be used as a test set. 3 graders graded the 270 images after being trained. A grade of 1 indicated normal and intact epithelium with no evidence of structural damage or fluorescein dye leakage. Grade 2 represented a partially damaged epithelium with no evidence of overt structural damage but may have some dye leakage. Grade 3 represented significant exfoliation of the surface epithelium and loss of barrier function. Gross leakage of fluorescein dye was seen on grade 3 images. The study resulted in a significant difference seen between the BZK treated images and the untreated control images. The mean grade for untreated images was 1.19 (SD 0.53) and mean for the BZK treated images was 2.55 (SD 0.75). The kappa value was 0.797, indicating that the graders had good agreement on scoring.

This study showed that confocal endomicroscopy is a reliable method for assessing structural damage and alterations in permeability in colonic mucosal epithelium cells. This study proved that the method is reliable for use in assessing local microbicidal agents that perturb the mucosal epithelium. The next step is to further develop this imaging modality for use in other applications such as irritable bowel syndrome and the assessment of gut permeability when exposed to agents other than BZK. The damage caused by BZK is significant. Further studies are necessary to determine if endomicroscopy can detect more subtle alterations, and to validate CE as a measure of permeability. The results demonstrated in this study were recently published in peer reviewed publication (38).

INTRODUCTION

Increased permeability of the gut is an underlying mechanism in the pathophysiology of several disease states, most notably irritable bowel syndrome and leaky gut syndrome. Increased paracellular or transcellular permeability allows the contents of the gut lumen to move through the normally protective epithelial mucosa and into the tissue of the gut (16). Luminal contents can include bacteria and other pathogens that may cause an inflammatory response in the lamina propria of the gut. Conditioning of the gut to respond to normal gut flora in this way may lead to autoimmune gastrointestinal diseases. In a clinical study of patients who meet diagnostic criteria for irritable bowel syndrome, 50% of patients exhibited increased gut permeability (17). Due to the potential cyclic nature of IBS, there is potential for more than 50% of patients to actually have increased permeability. The surface mucosal permeability is of particular interest, but the characterization of interstitial damage and permeability is also valuable.

Sub-surface permeability and damage may assist in the characterization of inflammation in the lamina propria.

Various measures of gut permeability exist that can be applied in the clinic and in the laboratory setting. Some methods measure whole-gut permeability and others are more localized measurements. The currently used clinical test for whole-gut permeability is the lactulose/mannitol absorption study (39). Lactulose and mannitol are administered orally in a mixture with water. Lactulose is absorbed paracellularly throughout the gut in trace amounts in normal subjects (39). Inflammatory conditions such as inflammatory bowel disease or celiac disease can damage the junctions between cells and increase the quantity of lactulose that is absorbed during the test. The majority of mannitol absorption occurs transcellularly, making it an ideal control comparison to lactulose absorption. Lactulose and mannitol are each absorbed as they move through the gastrointestinal system. Their absorption moves them into the vascular space, where they are filtered by the kidneys and excreted without undergoing metabolism. Urine or blood collection is performed frequently over a fixed amount of time after the initial administration of lactulose and mannitol. Earlier collection times correspond to absorption that has occurred more proximally in the gut. Later collection times are more distal sites, with 6-8 hour collection being due primarily to colonic absorption (18, 39). It is noted for study purposes that this temporal sequence may shift in different species in which slower or faster motility times are present. Even among human patients, there may be significant variability in gut transit times. After collection is complete, the ratio and absolute amount of lactulose and mannitol may be used to determine gut permeability. Increased lactulose

absorption with relatively stable mannitol absorption may be indicative of inflammation and destruction of tight junctions and other paracellular adhesions (39).

Alternatives to whole gut permeability testing exist but they typically utilize similar principles. 51Cr-ethylenediaminetetraacetic acid (EDTA) can be used as an alternative to lactulose for measuring paracellular permeability (39). Other alternatives exist, but lactulose and mannitol are cost effective and easy to administer, and so they are the most commonly used testing agents. Localized gut permeability is measured in a different way than whole-gut permeability. Tissue specimens from specific sites can be measured using a Ussing chamber. This is a well-tested method that can be used to study the transport of nutrients and ions across epithelial surfaces by utilizing two chambers with different ion concentrations (39). Flux is measured to determine permeability. While this test measures permeability reliably and reproducibly, Ussing chambers require fresh intestinal specimens, making sacrifice of the animal the most practical way to accomplish this test. Using human material is very difficult, making it an impractical test for clinical use.

Confocal endomicroscopy is a potential method to measure local gut permeability in a minimally invasive way when compared to the Ussing chamber method. No biopsy specimen is needed, and images can be analyzed real time during the procedure to assess permeability. Intravenously administered fluorescein dye is given and allowed to permeate throughout the body. CE is performed at the site of interest to assess for the presence of fluorescein leakage through the tissue (38). Gut mucosal tissue that has been damaged will allow fluorescein dye to leak into the luminal space, where it is easily observable with CE. Fluorescein is not transported transcellularly, so any leakage seen is

a result of paracellular or gross gaps in the epithelium, in a similar manner to lactulose permeability in the lactulose/mannitol absorption study. In some studies, acriflavine or other dyes are additionally administered. Acriflavine is applied locally to provide contrast to the surface of the epithelium, aiding in the identification of sub-cellular structures. However, when permeability is being tested, fluorescein is the only dye needed.

Damage to the colonic mucosal epithelium can lead to increased susceptibility to infection, disease, and other sequelae. Mucosal damage with barrier disruption and increased permeability is a theorized pathophysiological mechanism for gastrointestinal diseases such as irritable bowel syndrome (40-42). In a clinical study of patients with IBS, over 50% had increased permeability when undergoing the lactulose/mannitol permeability test (17). Barrier disruption and the risk of chronic inflammation are also concerns in inflammatory bowel disease (40, 43). Continued epithelial inflammation can lead to dysplasia, increasing the risk of colorectal cancer in IBD. In particular, ulcerative colitis causes chronic rectal inflammation of such severity that early screening colonoscopy is required to provide surveillance for colorectal cancer (1, 3, 10). Mucosal damage may additionally disrupt the microbiome that normally protects the colonic epithelium (44, 45). Shifts in the microbiome can lead to increased susceptibility to transient infections such as *Clostridium difficile (44)*. These infections can be difficult to treat and can cause chronic diarrhea.

In addition to causing transient infections, mucosal damage can increase susceptibility to long-term infections such as HIV. HIV and other pathogen infections are more likely to occur across the rectal mucosal barrier after injury to the mucosal surface (28, 29, 33). Injury to the mucosal surface can occur due to various methods: disease

states causing inflammatory changes, mechanical forces such as shearing, or topical chemical agents such as microbicides and lubricants. Recent studies have shown that damage to the rectal mucosa can increase the risk of transmission of HIV by facilitating translocation of the virus from the rectal lumen into the tissue (35-37). However, there is still a fundamental lack of understanding of the full effect that mucosal damage can have in disease susceptibility.

Existing studies on chemical perturbation of the rectal mucosa, with a specific focus on microbicide and lubrication agents, have included *in vitro* cell culture with testing of agents, lavage collection of fluids for cellular analysis, and use of *ex vivo* rectal tissue explants from humans (46, 47). These techniques have provided the groundwork for testing microbicidal agents such as nonoxynol-9 and benzalkonium chloride. These methods have studied the structural effects of these agents and shown that mucosal structure is disrupted at varying concentrations of microbicidal agents (48-50). However, structural integrity testing must be accompanied by functional testing to provide a complete assessment of the effect of each test agent.

More recent studies have utilized advanced *in vivo* imaging techniques to work towards simultaneous structural and functional testing. Optical coherence tomography with accompanying colonoscopy performed in sheep utilizing 0.2% BZK solution and control PBS revealed significant disruption of mucosal structure with BZK treatment (50-52). This was assessed with a visual scoring system and confirmed by biopsy and histological assessment. In addition, assessment by white light colonoscopy showed similar results, with BZK causing visible damage to treated areas. Fuchs et al. provide a model for testing function of the rectal mucosal tissue when exposed to nonoxynol-9 by

utilizing Technetium labeled DPTA (37). This provides a measure of rectal permeability as urine is collected over 24 hours and analyzed to determine concentration of DPTA. This radioisotope method successfully identified a state of increased permeability in subjects treated with nonoxynol-9.

Despite these recent advances in the assessment of structure and function of rectal mucosa with exposure to microbicidal chemicals, there is still a need for a method to combine both structural and functional assessment of mucosal surfaces. Confocal endomicroscopy represents a potential solution. This imaging method has already been utilized in the assessment of gastrointestinal diseases. It is an accepted clinical method to assess epithelial metaplasia in the context of Barrett's esophagus, providing a minimally invasive method for rapid evaluation of potential lesions (6). CE is also used in assessment of inflammatory bowel disease with a goal to predict potential flares (10). CE can be extended for use in the evaluation of microbicidal agents to help prevent HIV transmission. Better testing is required of microbicidal agents; despite microbicidal effects that may aid in destruction of potential pathogens, care must be given to ensure that these agents are not also destroying the mucosal epithelium to a degree which is inherently less beneficial than not using a microbicidal agent. The structural image data provided by confocal endomicroscopy may also provide additional insight into the inflammatory process in several disease states. The visualization of leukocytes and lymphocytes by CE could characterize the inflammatory response in pathogen infection, wound healing, or gastrointestinal disease (53, 54).

This study aims to assess CE as a method to evaluate *in vivo* rectal tissue when exposed to a microbicidal test agent, BZK. CE will provide both structural and functional

27

information in real time with the aid of fluorescent markers to aid in tissue delineation and permeability evaluation. In addition to evaluating agents that may alter HIV susceptibility, this study provides information on CE as a method to evaluate structure and functions such as leukocyte response to injury for application to other gastrointestinal diseases (38).

MATERIALS AND METHODS

This study complied with all appropriate IACUC rules and regulations on animal experimentation and was reviewed by the board at UTMB before implementation. 6 Merino sheep weighing 25-35kg were used. They were kept on a strict 12-h light and 12-h dark cycle and fed twice daily. The sheep were fasted the night before experimentation. Anesthesia for this procedure was 10 mg/kg of intramuscular ketamine, 10 mg/kg of intravenous ketamine, and 0.1 to 0.2 mg/kg of diazepam. The sheep were positioned in the dorsal supine position throughout the procedure.

Imaging was performed with an Optiscan FIVE1 laser scanning confocal endomicroscope. The probe is 5 mm in diameter and 30 mm in length. Light is provided by a 488 nm argon ion laser with collector set to 505-750 nm. Frame size is 475 x 475 μm and endoscopy is performed at 0.7 frames per second. Throughout the procedure, different sites were assessed to provide diversity of test images. At each site, an average of 25 images were taken to ensure quality of final chosen images. Two fluorescent labeling probes were utilized. 0.05% acriflavine in saline solution provided local surface barrier microarchitecture staining with subcellular delineation. 500mL intravenously administered fluorescein dye was given along with 250 mL of saline at an infusion rate of 3 mL/min throughout the fluorescein imaging portion of the procedure. Fluorescein was

given for functional assessment of barrier permeability. After initial administration of fluorescein dye, imaging was delayed for 2 minutes to allow for systemic infusion. Images were obtained in the sigmorectal region in multiple imaging regions circumferentially. Biopsies were similarly obtained in multiple regions after completion of imaging for histological assessment.

The imaging procedure was initiated by obtaining baseline background images with no fluorescent probe. These images contained no detectable signal but are used for background subtraction during analysis if necessary. After baseline imaging, acriflavine was introduced topically and was allowed to permeate the rectal cavity for 5 minutes before excess acriflavine was rinsed with PBS. Imaging was performed regionally in 4 regions. These were the anterior surface, posterior surface, and each of the lateral walls of the rectum. Each imaged area was approximately 2 cm proximal to the anorectal verge. A variety of sites were imaged in each region to fully assess rectal mucosal microstructure before BZK. After acriflavine imaging, fluorescein infusion was begun. Each region and site were again imaged after the fluorescein probe was introduced to assess baseline functional permeability.

Injury to the mucosa was induced by introducing a sterile rectal swab soaked in 0.01% BZK solution 2 cm past the anorectal verge to the imaging region and kept in contact with the mucosa for 5 minutes before removal. After application of the BZK solution, the rectum was rinsed with PBS to remove excess agent. Imaging was then performed regionally in the same manner as with the fluorophore-only imaging.

The images were scored based on a previously accepted confocal imaging grading standard (10). This system was modified to include both the structural assessment

provided by the acriflavine dye and the functional permeability assessment from the fluorescein dye. This technique builds on Kiesslich et al's grading system where only fluorescein dye was utilized. 370 images obtained from the six sheep were randomized to be graded. The first 100 randomized images were used as a training image set for each of the 3 graders. The 3 point grading system modified from Kiesslich was used to identify structural disruption as well as functional permeability. Features of the grading system are provided in Table 2.1. A grade of 3 represents severe disruption of the epithelium while a grade of 1 represents undamaged tissue. Each of the 3 graders evaluated the set of 270 test images and scored each image. Fleiss's K was utilized to evaluate agreement between the set of 3 graders. The images treated with BZK were compared to control, undamaged fluorescein and acriflavine dye only images. Statistical analysis between groups was evaluated by the Mann-Whitney U test with a P value of <0.05 considered to be significant.

To confirm the findings of CE, biopsies were taken and stained with H&E and graded for structural disruption and inflammation. The criteria by which the biopsy specimens were graded were as follows: inflammation (0 or 1), edema of the lamina propria (0 or 1), epithelial disruption or detachment (0 or 1), presence of microabcesses (0 or 1), and hemorrhage (0 or 1). Scores were summed with a higher score representing increased mucosal damage. This scoring system is consistent with previous studies (10). For each sheep, 4 to 6 biopsy specimens were obtained, with 5 fields per section examined for grading. In addition to grading, epithelial denuding was evaluated quantitatively using image processing software (ImageJ, NIH Image) by using line

segments to delineate areas of epithelial damage. The overall percent of epithelial

disruption was determined by the ratio of denuded length to total length.

Grade	Criteria
1	Ordered arrangement of the gland
	Intact layer of columnar epithelium
	No microstructural damage
	Glands round or elongated
2	One, some, or all lumens of the crypts filled with fluorescein
	No microstructural damage
	Flooding of fluorescein (between the crypts) less than 25%
3	Exfoliation in the cellular structure
	Disruption in crypts
	Excessive flooding

Table 2.1:   Grading criteria for CE scoring (38)
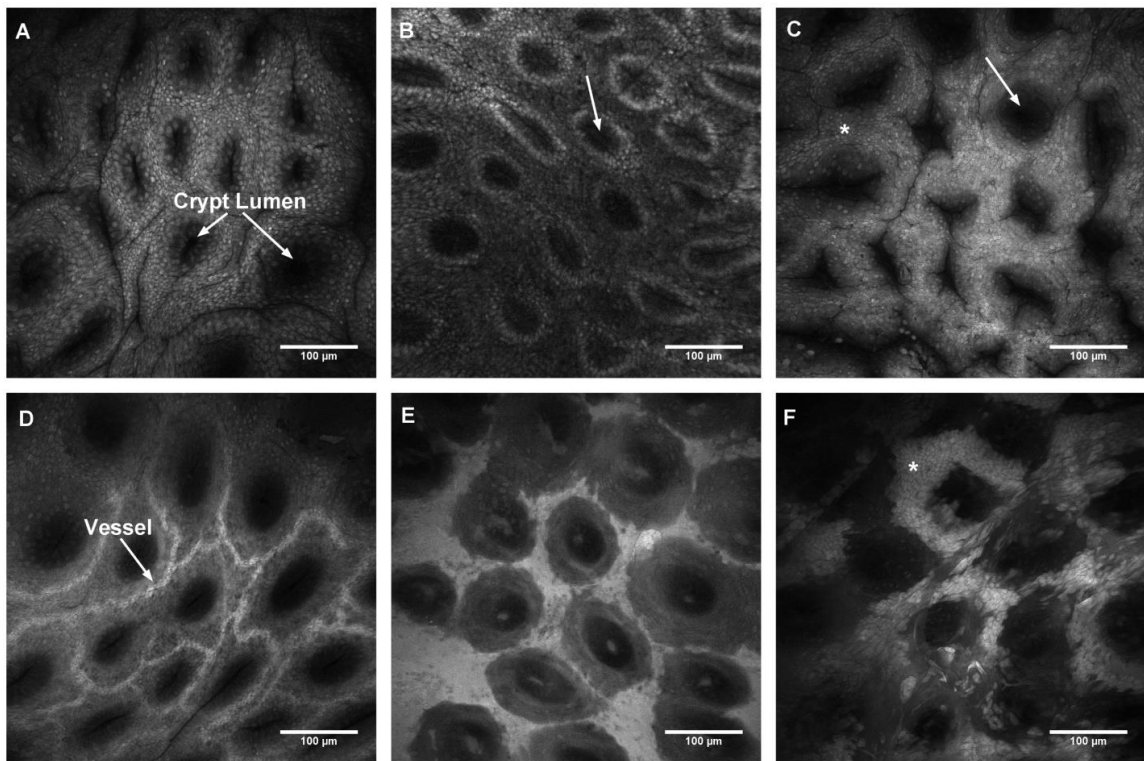
Figure 2.1:   Images obtained using confocal endomicroscopy (38)

RESULTS

Images obtained using CE are shown in Figure 2.1. Normal rectal mucosa stained with acriflavine shows microstructural cellular organization with the nuclei of the cells visible, and can be observed in Figure 2.1a. Columnar epithelial cells line the entire mucosa, with occasional goblet cells seen in the region of the crypts. Goblet cells appear slightly larger than other surrounding cells and are responsible for secretion of mucus onto the epithelial surface to help maintain the epithelial barrier. As indicated by the arrow in Figure 2.1b, crypts are typically visible as round dark regions with cells appearing in a slightly different orientation due to differences in depth. Crypt architecture can appear variable in CE images due to the angle at which the probe tip contacts the mucosal surface. Folding or flattening of the crypts can occur with varied angles and with varying pressure applied by the probe operator. Beyond the cell surface, the lamina propria becomes easily visible only with the introduction of fluorescein staining. The topically applied acriflavine does not permeate at depth to provide sub-surface imaging contrast. Figure 2.1c shows the surface epithelium following fluorescein dye administration, with the arrow again indicating a crypt. Fluorescein dye is visible within the vasculature and appears as bright concentrated lines, as shown in Figure 2.1d. Blood cells may become visible within the vasculature in some images.

The introduction of 0.01% BZK causes readily apparent damage to the mucosa. Fluorescein can be seen leaking into the lumen, and will pool in the bottoms of the crypts. The accumulation of fluorescein occurs both between the crypts and at the bottom of the crypts, as is seen in Figure 2.1e after BZK application. This caused a loss of crypt architecture as increased volumes of fluorescein leak through the epithelium. In addition

to leakage, cellular debris may be seen as the columnar epithelium is denuded and these cells were released, as shown in Figure 2.1f. Gaps may be seen in the epithelial surface between crypts which represent epithelial cell gaps due to shedding. It is noted that gaps may be visible normally, but that the introduction of a chemical agent such as BZK increases the cell shedding. In severe damage, entire regions of the epithelium may be lost. In pilot testing for this study, higher concentrations of BZK were utilized which resulted in swift denuding of large regions of epithelium with little variability. A lower concentration was utilized in this study to evaluate more realistic doses seen in microbicidal products as well as to offer more variety in the degree of damage observed. Different regions may be variably damaged, leading to the broad range of features seen in BZK treated images in this study. As was shown in Table 2.1, moderately damaged images received a score of 2 whereas severe damage received a score of 3. In addition to the features highlighted in Table 2.1 and utilized in the grading system, there are other observable effects of BZK treatment and mucosal damage.
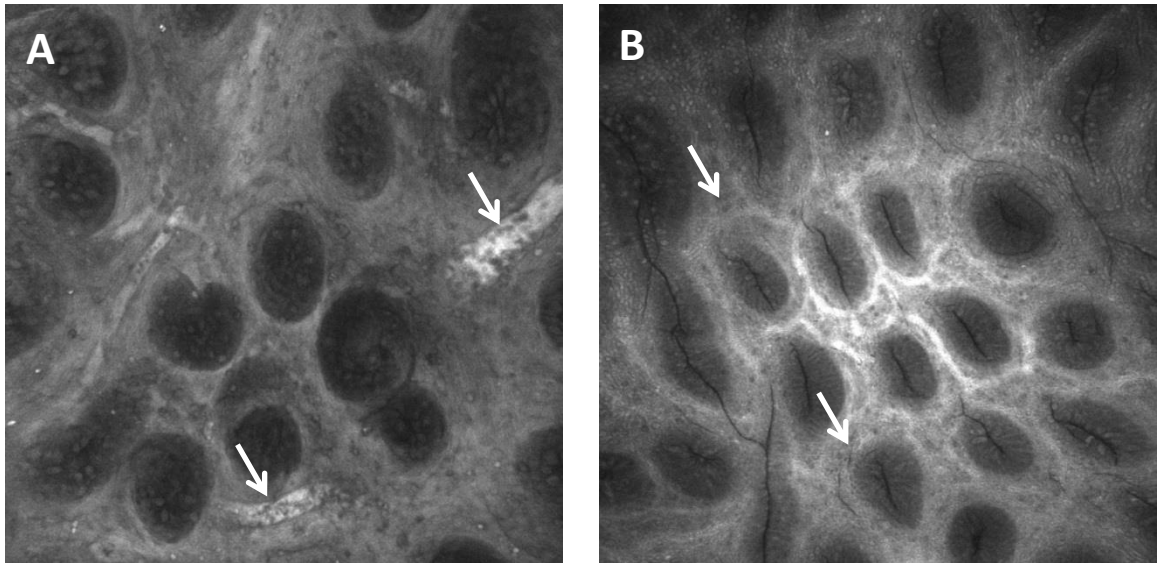
Figure 2.2:   Leukocytes visible in vessels and lamina propria responding to injury

Leukocyte aggregation at BZK treated sites are often observed as dark gaps in deeper sections of the mucosa. These leukocytes are quickly extravasating from the vasculature to aggregate at points of damage to regulate the inflammatory response. The presence of these leukocytes can be observed in Figure 2.2. It is important to differentiate between epithelial cell gaps that occur as dark spaces in between stained epithelial cells, and these leukocytes which occur in images taken at depth in the lamina propria. Figure 2.2a shows the intavascular leukocytes within larger and smaller vessels below the surface in the lamina propria. The arrows in Figure 2.2b indicate the perivascular leukocytes that have extravasated from the adjacent blood vessel. These cells are responding to the inflammation and injury caused by the BZK damage. Leukocytes responding to the injury will release inflammatory mediators to clear the damaged epithelium and begin healing. However, it is challenging to identify the specific type of leukocytes visible on CE. The well vascularized gut mucosa allows a fast immune

response. The images in Figure 2.2 were taken only minutes after BZK damage was induced. Preliminary image analysis performed on images from BZK treated and untreated tissues revealed a wide variation in the number of leukocytes present. Images from both groups ranged from having few to no leukocytes to having large leukocytes aggregations noted. It proved difficult to accurately count the number of leukocytes and compare between each group. Additional data may be required to more fully characterize the role of leukocytes in response to BZK treatment and wound healing as visualized by CE.

Figure 2.2 also provides a view of another effect that BZK treatment has on the structure of the epithelium. Normal epithelium has readily visible goblet cells in each crypt. These cells appear to be oblong and are larger than surrounding cells. However, as noted in the crypts in Figure 2.2b, BZK damage is associated with significantly less goblet cells visible within the crypts. The crypts in the center of Figure 2.2b show scant goblet cells, while some of the more peripheral crypts show some goblet cells. Goblet cells may be particularly vulnerable to shedding with mucosal injury such as that provided by BZK treatment.
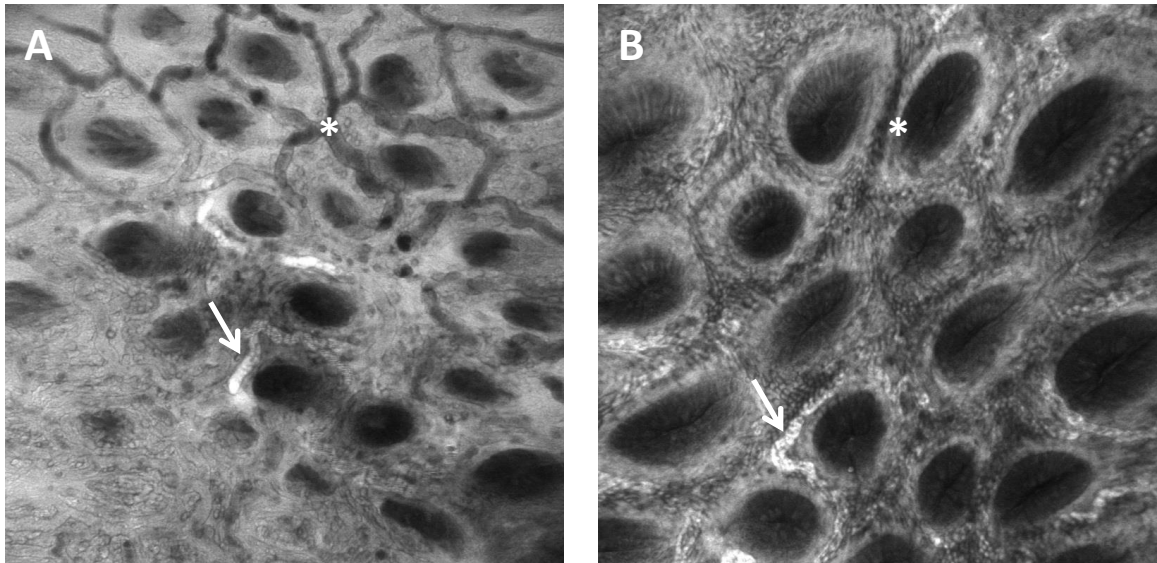
Figure 2.3:   Variations in vessel architecture and fluorescein concentration after BZK

Fluorescein dye is administered intravenously and distributes throughout the vascular system in the body. The fluorescent nature of the dye causes blood vessels to appear as brightly contrasting areas in the tissue. An example of the typical appearance of blood vessels is seen in Figure 2.1d. This appearance is typical in both untreated images and in images in which BZK has been applied. However, BZK treated samples can also have a variant in the apparent appearance of the vasculature. As is shown above in Figure 2.3, vessels may take on a darker appearance with fluorescein dense areas alternatively appearing as concentrated bright segments. The arrows in Figure 2.3 indicate blood vessels. The stark transition from darkened vessels to brightly concentrated vessels is not typically seen. The revelation of these darker vessels in BZK treated areas has several potential explanations. The aggregation of lymphocytes to the perivascular space may be responsible for some part of this mechanism, as the lymphocytes appear dark when in the vasculature and after extravasating into the surrounding tissue. Another contributing

factor may be damage to superficial capillary vessels with concentrated leakage of fluorescein dye that is seen leaking out onto the surface of the epithelium. The relative depth difference between this superficial dye and the other undamaged and deeper vessels results in a difference in intensity seen between vessels. Finally, the presence of lymphatic system must be considered. Lymphatic vessels are responsible for the transport of fats from the intestines to the systemic circulation. Lymphatic vessels have their origin in the intestines and fluorescein dye may be taken up by the lymphatic system. The lower concentration of fluorescein in these vessels when compared to the vasculature may account for the findings shown in Figure 2.3. These vessels are indicated by stars in Figure 2.3.

Figure 2.4 shows example images of the confocal and histologic grading system used, with the criteria described in Table 2.1 and above. Panels a and d correspond with a grade of 1, indicating minimal or no damage. Panels b and e indicate a grade of 2, with partial damage noted. There is fluorescein visible in the confocal image but it is limited. A portion of the epithelium has been denuded and is visible on the histological image in panel e, but portions of the epithelium remain intact. Panels c and f correspond with a grade of 3, and show extensive damage. Epithelial cells that have been shed from the surface are seen aggregating. Fluorescein is visible over the majority of the image, indicating a large increase in mucosal permeability. The histological section in panel f shows complete denuding of the epithelium. Crypt architecture and goblet cells are easily seen in panel d, but are not easily recognizable in panel f.
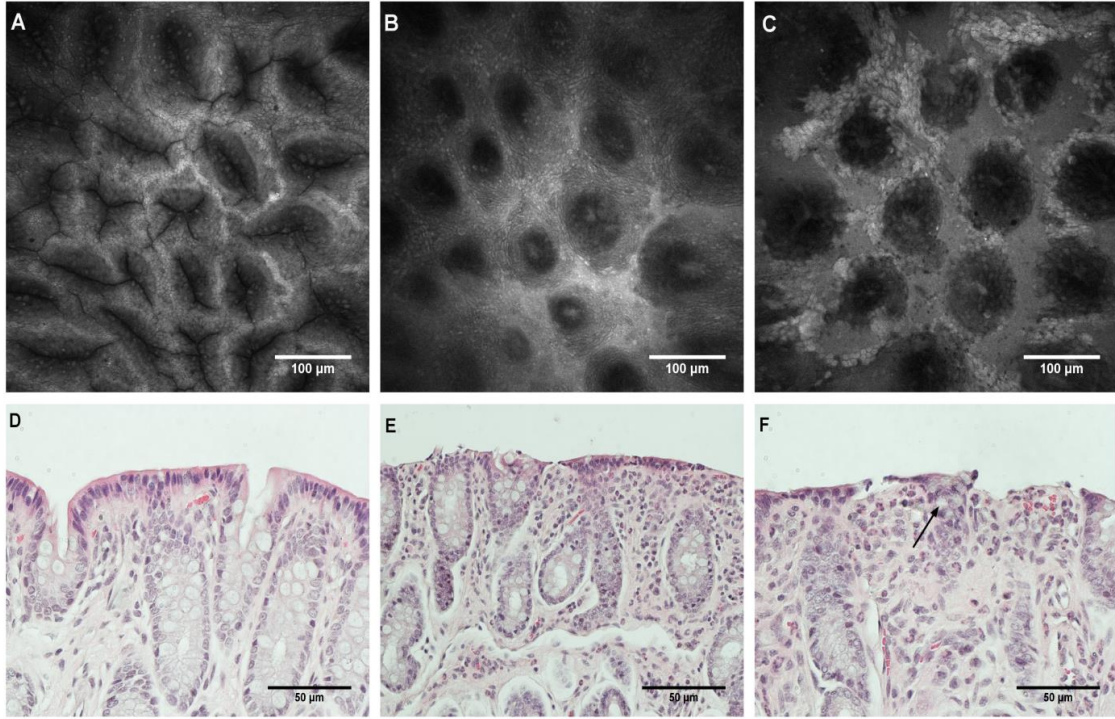
Figure 2.4: Representative confocal and histological grading images (38)

The results of the CE and H&E grading are shown in Figure 2.5. The mean CE grade for untreated images was 1.19 (SD 0.53) and the mean grade for BZK treated images was 2.55 (SD 0.75). Fleiss' Kapppa value for the agreement between the three individual graders was 0.797, indicating excellent agreement between each of the graders. The mean grades are significantly different with a P value of < 0.05. Histological grading results are shown as well in Figure 2.5. Untreated sites had a mean grade of 1.75 (SD 0.35) and BZK treated sites had a mean grade of 2.68 (SD 0.39). The difference in mean grade for H&E is also significant.
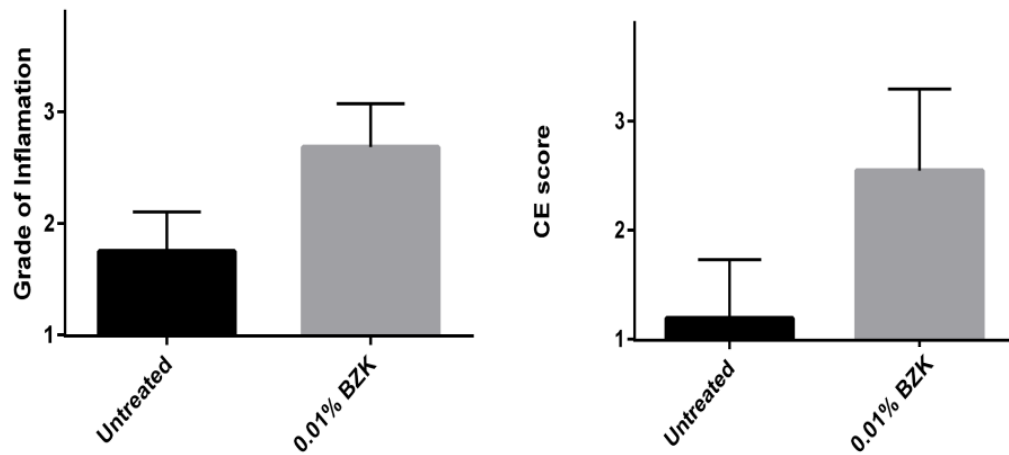
Figure 2.5:   CE and H&E grading results (38)

DISCUSSION

The need for a method that has the capability to evaluate epithelial surfaces and combines structural evaluation with functional assessment is apparent. Disruption of epithelial mucosal surfaces is linked to increased risk of infection by various pathogens as well as susceptibility to other gastrointestinal diseases. In particular, methods are needed that can potentially provide structural and functional measures in real time in clinical patients in the future. This study evaluates confocal endomicroscopy as a method for evaluating rectal mucosal damage in an ovine model. CE provides subcellular structural imaging with the assistance of appropriate dyes as well as a real time functional permeability measure to evaluate mucosal leakage.

CE scoring using a two dye combined approach corresponded well with histological grading. Both histological and confocal scoring systems indicated significant structural damage to the mucosa with BZK treatment. CE was also able to indicate an

increased permeability with BZK treatment. Permeability assessment by this scoring system provided a basic method of assessment but there exists a need for more quantitative methods of permeability assessment when utilizing CE and fluorescein dye. It is noted that there are untreated images in which trace fluorescein leakage can be seen. Natural epithelial cell shedding occurs regularly, with the entire epithelium being replaced approximately every 3 to 5 days. Due to this natural shedding, there are often cellular gaps in the epithelium. These gaps may be responsible for the trace leakage that can be seen in untreated images. In addition to cellular gaps, there may be paracellular disruptions that allow for fluorescein leakage. Tight junctions and adherens junctions may be allowing trace leakage. Further testing is needed to assess the tight junctions of the epithelium and to correlate CE observed leakage with tight junction expression in the mucosa.

Leukocytes and lymphocytes are observed in many of the CE images gathered in this study, but no apparent trend emerged. There were images where leukocytes were easily identifiable but many others where none could be observed. These cells may be temporally observed, with an increased aggregation of immune cells likely occurring as time from BZK damage increases. Further testing is needed to ascertain the role of CE in evaluating immune cell aggregation and response to mucosal injuries. As immune response and other observable aspects in CE are more thoroughly investigated, additional information will become available that may be included in more advanced scoring systems. In particular, the use of an additional fluorophore that selectively highlights leukocytes such as rhodamine 6-G may allow for direct visualization in real time of leukocytes rolling and extravasating in response to injury. In the assessment of HIV

susceptibility, CE is only beginning to be used to its full potential. Future directions for study should include varying the concentration of BZK used, as well as evaluation of alternative microbicidal agents. These variations may be combined with immune measurements to gather a more complete understanding of the altered pathogenesis and transmission of HIV in damaged rectal mucosa. Ultimately, lubricants and microbicidal agents should be designed to prevent transmission rather than aid it.

Another area of potential future study is the further characterization of the role of lymphatic vessels in permeability and on fluorescein dye leakage in the gut mucosa. Figure 2.3 identified potential lymphatic vessels in the current study. The lymphatics likely play a part in transporting fluorescein that has moved out of the vasculature. As the lymphatics absorb nutrients that have been transported across the gut mucosa such as fats and cholesterols, fluorescein may also move into the lymphatic vessels. It may be of use to attempt to inject fluorescein or another dye into the lymphatic system selectively to attempt to further characterize the role of these vessels in permeability models of the gut.

CE may also be further developed for use in the evaluation of gastrointestinal diseases such as inflammatory bowel disease, irritable bowel syndrome, and cancer. The use of a two dye system of acriflavine plus fluorescein allowed increased capability in this study that may be extended to other applications. The addition of acriflavine to fluorescein for the prediction of flares in Crohn's disease may improve outcomes if implemented. Irritable bowel syndrome is currently diagnosed solely on clinical criteria, without a corresponding empirical for diagnosis. CE may be a potential diagnostic tool that could aid in identifying microstructural damage and alterations in local permeability

to aid in IBS diagnosis. Further study is necessary to ascertain CE's role in diagnosis and to better understand the underlying pathophysiology of IBS in general.

This study utilized confocal endomicroscopy as a method for assessing both structure and functional permeability of damaged mucosal surfaces. CE reliably demonstrated that BZK significantly disrupts both structure and function of the rectal mucosa. This ovine model is anatomically and physiologically similar to humans and this study is applicable to humans. CE provided a minimally invasive method of assessment that may be utilized in the clinic. Further studies are required to more accurately assess the immune response to localized injury in the colon, to provide a quantitative measure of functional permeability, and to validate CE as a method for measuring permeability.

Chapter 3 Quantitative analysis of confocal endomicroscopic images to assess colorectal epithelial permeability by texture analysis

SUMMARY

Various methods exist for the measure of permeability of mucosal epithelial surfaces, such as the lactulose/mannitol absorption test and the Ussing chamber method. These methods are reliable, but there is a need for a localized permeability measure that can be applied cheaply and ideally in conjunction with procedures such as colonoscopy. As discussed in the previous chapter, confocal endomicroscopic imaging of mucosal surfaces after the administration of intravenous fluorescein dye is a potential method for assessing local permeability.

This study improves on existing grading scales by adding a quantitative method of analysis based on the grey level co-occurrence matrix (GLCM) texture analysis method. Using this method, the correlation statistic was determined to provide a quantitative measure of permeability. Application of this test statistic to a set of 44 test images resulted in correct identification of increased permeability in BZK treated tissues with a sensitivity of 95.5% and a specificity of 95.5% as well. Further studies are needed to compare this method against other permeability measures and to expand this quantitative analysis for use in a ordinal scale of variable permeability measures.

INTRODUCTION

Current methods for evaluating mucosal permeability based on fluorescein administration and CE imaging rely on a visual grading system (10, 38). This grading system has been modified several times to allow for various applications. Most recently,

it was adopted to measure altered rectal permeability with application of chemical microbicides with the goal of characterizing microbicide effects on pathogen transmissibility. Fluorescein was administered intravenously and allowed to fully permeate the vascular space. CE was used at the area of interest to capture images of leaking fluorescein. Images were graded on a scale from 1 to 3, with 1 being undamaged tissue and 3 showing severe damage. A grade of 2 indicated pooling of fluorescein in the rectal crypts, but less than 25% of the space in between crypts covered in fluorescein. Fluorescein preferentially pools in crypts due to the depression below the surface. It is not clear if crypts are more easily damaged and are preferentially damaged over areas in between crypts. A grade of 3 on this scale indicates severe damage with fluorescein covering potentially the entire field of view.

Despite the reliability of this current grading system, there is a need for a more quantitative method to measure mucosal permeability when utilizing the fluorescein and confocal endomicroscopy method. Quantitative image analysis methods exist for various grading of confocal images and have been used in various applications. It has been used to evaluate cervical neoplasia by analyzing features such as cell density, the morphology of the nuclei, and other features of tissue architecture (55). In addition, quantitative analysis of CE images has been used intraoperatively in neurosurgical applications for better determination of surgical margins (9). However, these methods are focused on cellular features and were not designed for use with fluorescein dye for a quantitative method of permeability.

Texture analysis via grey level co-occurrence matrix analysis is a well-known technique of image analysis that has been applied widely. Analysis is based on building a

matrix of statistical features of the various grey levels over the entire image (56). These statistics are used to calculate summary statistics such as entropy, contrast, and correlation for the image. These measures can be compared and used to develop an algorithm for determination of pathology for a particular image (56).

The purpose of this study was to develop a method for quantitatively analyzing confocal endomicroscopic images of the rectum in an ovine model to determine whether images were from areas treated with BZK to induce damage, which corresponds to an area of increased permeability. Images of tissue treated with BZK with increased permeability were compared to undamaged images with unaltered permeability. Grey level co-occurrence matrix analysis was performed on a set of test images to develop a method for determining permeability of mucosal surfaces.

Category	Criteria
BZK treated, increased permeability	BZK treated tissue Fluorescein pooling in crypts or on surface of epithelium No cellular debris or dye on the probe tip Image must be in focus Image must be from the surface One image per site
Non-treated, non-permeable	No fluorescein visible in the image No cellular debris or dye on the probe tip Image must be in focus Image must be from the surface One image per site

Table 3.1:   Image inclusion criteria

MATERIALS AND METHODS

This study complies with all appropriate IACUC rules and regulations on animal experimentation and was reviewed by the board at UTMB before implementation. Images obtained for this study were from Merino sheep weighing 25-35 kg. They were kept on a

strict 12-h light and 12-h dark cycle and fed twice daily. Imaging was performed with an

Optiscan FIVE1 laser scanning confocal endomicroscope. The probe is 5 mm in diameter

and 30 mm in length. Light is provided by a 488 nm argon ion laser with collector set to

505-750 nm. Frame size is 475 x 475 µm and endoscopy is performed at 0.7 frames per

second, with a resolution of 1024 x 1024 pixels. Throughout the procedure, different sites

are assessed to provide diversity of test images.

Sheep were anesthetized and underwent imaging. 500mL intravenously

administered fluorescein dye is given along with 250 mL of saline at an infusion rate of 3

mL/min throughout the procedure. Animals were first imaged after fluorescein

administration to provide undamaged, low permeability images. 0.01-0.1% BZK solution

was applied locally to the rectum to induce injury and increase permeability. Imaging was

again performed after BZK application.

44 images were selected for analysis. The inclusion criteria for image selection

are included in Table 3.1. Images were not selected if the probe was not correctly focused

on the epithelial surface, or if the probe itself was covered in debris or dye which

obscured the underlying image. Imaging is done regionally to obtain multiple images at

the same site. Only one image from each site was included in this set of 44 test images.

Images were imported into ImageJ (NIH Image) and converted from 16 bit TIFF

images to 8 bit TIFF images. An artifact of the probe used produced dark areas of no

signal at the bottom of each image. A ROI was chosen that included only the upper 860

pixels of the 1024 x 1024 image to eliminate this artifact. Figure 3.1 shows an example of

this ROI on a sample image. The GLCM plug-in for ImageJ was run for each image to

provide values for angular second moment, contrast, correlation, inverse difference

moment, and entropy. The pixel step size was 1 and the angle 0 degrees. These features were analyzed and compared between the non-permeable and permeable images to determine which feature would be most predictive. Means were compared using the Student's t-test with a P value of < 0.05 as significant. After a feature was chosen, a cutoff value was chosen utilizing an ROC curve to choose the value with the best sensitivity and specificity for determining permeable images.
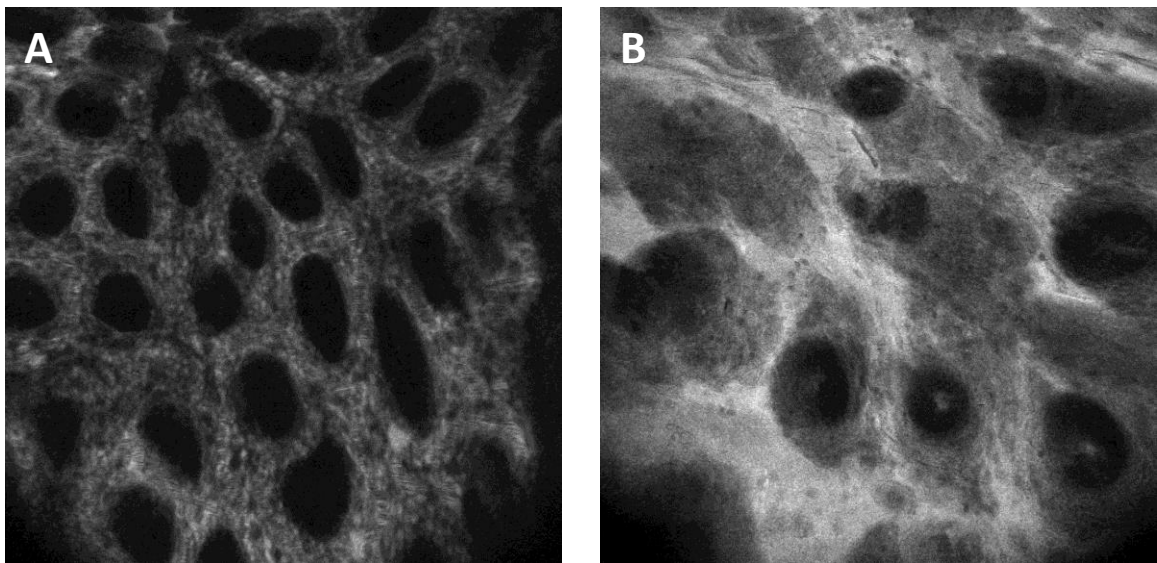
Figure 3.1:   Untreated non-permeable and BZK treated permeable representative
            confocal images

	Angular Second Moment		Contrast		Correlation		Inverse Difference Moment		Entropy	
	Mean	SD	Mean	SD	Mean	SD	Mean	SD	Mean	SD
Untreated non-permeable (n=22)	0.00046	0.00014	88.31589	48.24899	0.00134	0.00048	0.14559	0.03282	8.10284	0.31232
BZK treated permeable (n=22)	0.00031	0.00008	84.68970	25.54170	0.00072	0.00024	0.15235	0.03016	8.42737	0.19995

Table 3.2:   Mean results and SD for BZK treated permeable and untreated non-permeable images

RESULTS

Typical features of a BZK treated permeable and untreated non-permeable images can be seen in Figure 3.1. For image analysis, an ROI of 860 pixels in height and 1024 pixels in width was used to eliminate the areas of image attenuation at the bottom of each image. In Figure 3.1a, an untreated non-permeable, undamaged image is seen. Crypt architecture is readily visible, with dark spaces representing the crypts and lighter spaces between crypts representing the columnar epithelial surface. Goblet cells may be occasionally seen but are difficult to visualize with fluorescein dye alone. The visibility of the crypts may also change depending on the pressure of the probe being applied to the surface. Some images may contain crypts that have been flattened. Imaging at depth reveals the lamina propria with fluorescein visible in the vasculature. A more broad range of representative images can be viewed in Figure 2.1, but note that acriflavine was not utilized in this particular study, unlike the study performed in Chapter 2. In Figure 3.1B, an example of a damaged image with increased permeability is shown. Fluorescein can be seen pooling in the crypts as well as gathering on the surface. Large patches of white

represent these fluorescein regions. Some images may also have cellular shedding with free floating cells noted as well.

GLCM analysis revealed that the correlation feature proved to be the best for determining damage with corresponding increased permeability in the image set. Table 3.2 shows the mean of the results of each of the computed features in both the BZK treated permeable and untreated non-permeable group. Angular second moment did show a significant difference as well but as the obtained confocal images do not have a specific orientation, an angular measure is likely not reliable for differentiating images. The mean correlation value for the BZK treated permeable images was 0.00072 (SD 0.00024) and the mean correlation value for the untreated non-permeable images was 0.001335 (SD 0.000481). Using an ROC curve, the ideal cutoff point for differentiating the groups was determined to be 0.001005. Images with a correlation value higher than this value are classified as untreated non-permeable and images with a lower correlation value are classified as treated with increased permeability. The ROC curve is shown in Figure 3.2. This results in a sensitivity of 0.955 and a specificity of 0.955 as well. Choosing this cut-off point resulted in 1 permeable and 1 non-permeable image being misclassified by the algorithm.
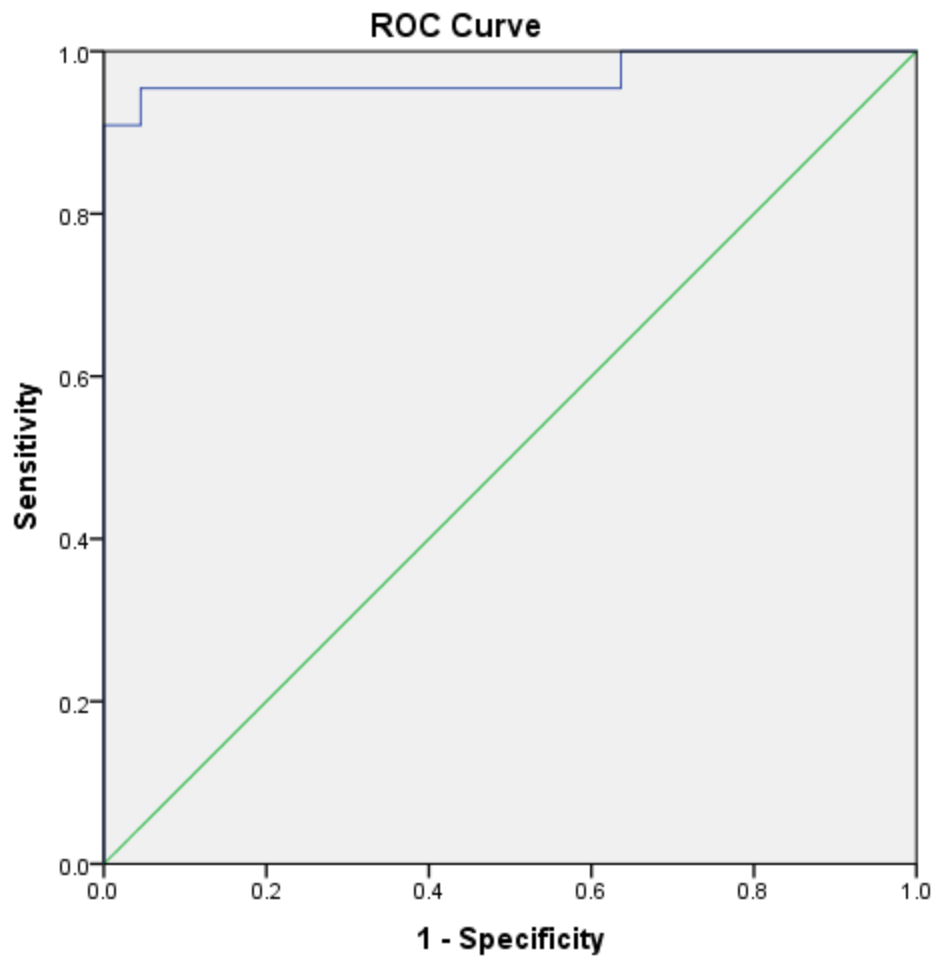
Figure 3.2:   ROC curve of treated and increased permeability cut-off result

Fluorescein dye given continuously through an intravenous route provided good contrast and was easily visible. It should also be noted that preliminary analysis of another image set that included the topically applied dye acriflavine showed very different results. After initial testing, it was determined that the acriflavine signal hinders the ability to properly assess fluorescein leakage. Surface acriflavine can mask underlying fluorescein and interfere with the ability of the GLCM plugin to differentiate treated permeable from untreated non-permeable images. After initial analysis, further

pilot testing was performed to determine the feasibility of performing GLCM analysis on

sub-surface image stacks for potential differences in tissue features that may be present

beyond leakage. CE is capable of imaging at depths of up to 70 μm but at the cost of

image quality. Figure 3.3 demonstrates the appearance of the epithelium as the image

depth is increased. It is of value to extend the capability of the currently developed

algorithm to sub-surface images in order to better assess tissue features that may differ

between groups such as inflammation that occurs in the lamina propria. In Figure 3.3a, it

is easily determined that there is increased permeability with fluorescein accumulation

both on the surface and in the crypts. The correlation value for this image was easily

below the cut-off value at 0.00049, making the image fall into the permeable category by

the algorithm. However, as the confocal microscope images deeper into the tissue, the

correlation value returned by GLCM increases and approaches the cutoff value between

permeable and non-permeable. In Figure 3.3, the value rises steadily between panels a to

d, with the correlation value of panel d right at the cutoff value at 0.001. Figure 3.3d is

not easy to correctly identify. The fluorescein leakage is not abundant, and there is no

pooling seen in the crypts. In addition, the ability to differentiate individual cells is

mostly lost. Moving to even deeper images further decreases image quality and does not

allow the GLCM analysis to accurately differentiate BZK treated permeable images from

untreated non-permeable images. Additionally, deeper image slices may contain

increased vasculature, which is not seen on the surface images. As a result of these

several confounding factors, the sensitivity and specificity of this analysis begins to fall

when imaging at depths below the surface. However, the use of GLCM may still be of

use at depth, as further analysis may reveal other texture features resulting from damage

due to BZK treatment, such as an increase in inflammatory response cells that may create

specific patterns.
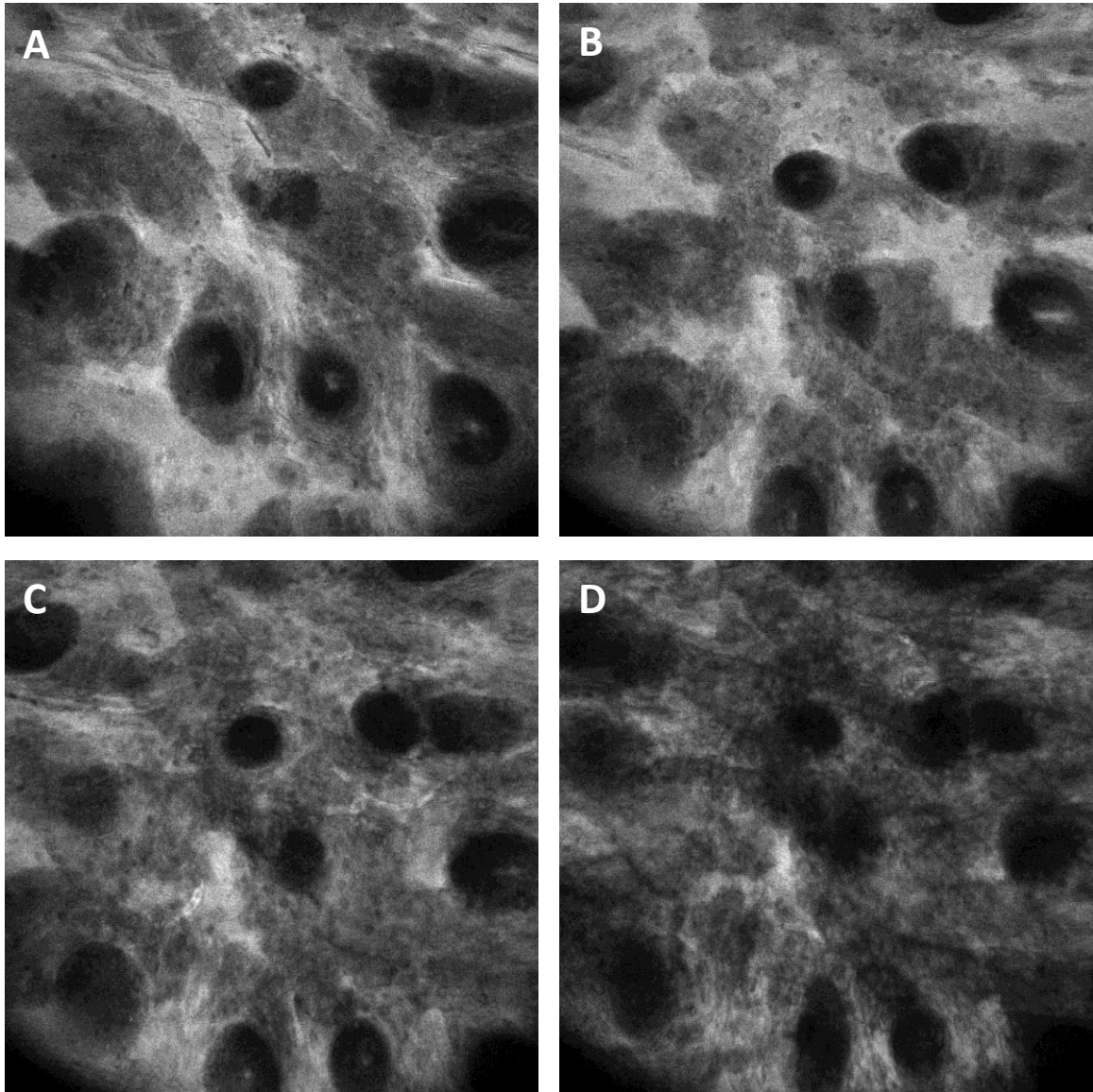
Figure 3.3:   Infusion of fluorescein dye seen at depth in BZK treated permeable and
              untreated non-permeable images

DISCUSSION

There is a need for a method of quantitatively assessing the permeability of

mucosal surfaces by utilizing fluorescein dye and confocal endomicroscopic imaging.

Existing methods of assessing localized permeability are invasive. The current grading

system for CE permeability relies solely on visual assessment by a grader. While the

Kappa value achieved in Chapter 2 between graders of 0.797 represents good inter-grader

agreement, this value still signifies a significant error rate in relying on qualitative

scoring systems for image evaluation. Ultimately, the quantitative assessment of

permeability developed in this study may have extensive applications in diagnosis of

diseases such as irritable bowel syndrome, leaky gut, and even guiding biopsy of

suspicious polyps on screening colonoscopy.

A method of analysis using GLCM texture features was developed to assess

images of varying permeability in the rectum in an ovine model. The correlation measure

was determined to be significantly different between the two groups and was chosen as

the best predictive statistic. The GLCM plugin calculates correlation by utilizing the

formula:

$$\sum_{i,j=0}^{N-1} P_{i,j} \left[\frac{(i - \mu_i)(j - \mu_j)}{\sqrt{(\sigma_i^2)(\sigma_j^2)}} \right]$$

Where $P_{i,j}$ is the entry into the normalized grey level spatial matrix, and μ and σ are the

means and standard deviations of P_i and P_j (56). This measure calculates the linear

dependency of each pixel on neighboring pixels. 0 is a perfectly uncorrelated image and a

measure of 1 would be a perfectly correlated image. Images with areas of homogeneity

will naturally have a larger correlation value as pixels in these regions will be correlated

with surrounding pixels. Images with significant homogeneity have high correlation statistics. In contrast to other methods, intensity measures are not utilized by this analysis method. In the CE images utilized in this study, non-permeable images had significantly higher correlation values when compared to permeable images. The non-permeable images appear more ordered with the crypts providing a pattern of homogeneity throughout the image. The black spaces of the crypts are areas that can be read with a high correlation value as each black pixel is predictive of surrounding similar black pixels. In contrast, the BZK treated permeable images are generally more disordered, with the standard crypt architecture disrupted. Fluorescein leakage is seen regionally in the image as well as pooling in the crypts. The disruption of the normal orderliness of the image creates significant heterogeneity. This corresponds to much lower correlation values than are seen with the untreated non-permeable images.

The ROC analysis provides the ideal cutoff value for applying the correlation of a test image to predict permeability. A cutoff value of 0.001005 provides a 95.5% sensitivity and a 95.5% specificity as well, indicating that the correlation statistic may be a promising method for assessing for permeability. It is important to note that the sample set was relatively small and that a larger set is needed to more rigorously test this parameter for predicting increased leakage. An increase in sensitivity with a correlated loss in specificity may be of interest when utilizing CE permeability as a screening method. This would further minimize the false negative rate at the expense of allowing more false positive tests. In the application of using CE permeability at suspicious lesion sites during colonoscopy, a highly sensitive screening is desirable. Any lesion that has increased permeability would then be subject to biopsy for further pathological

evaluation. Coupling of permeability measures with structural evaluation by a trained endoscopist may result in a significant reduction in the number of biopsy specimens required during routine colonoscopy. Previous studies already indicate that CE is a useful method of assessing structural features of colonic polyps and may assist in diagnosis (1, 2).

This application of the GLCM program to assess permeability currently functions only under a specific set of inclusion criteria as indicated in Table 3.1. Confocal endomicroscopy is capable of assessing tissue at depths extending into the lamina propria. However, as indicated in Figure 3.3, the GLCM correlation statistic provides decreasing sensitivity and specificity at greater depths. The image quality is decreased at depth and the plugin is not capable of distinguishing fluorescein that is contained intravascularly from fluorescein leakage at these depths. The heterogeneity of the vascular structure decreases correlation statistics of non-permeable images that are sampled at depth. This limitation may be addressed in future study by creating a more complex algorithm. While the vascular structures are inherently heterogeneous, they are arranged in linear patterns. Additionally, images which contain vasculature may have a higher contrast value than images without vasculature. Future study will be required to perfect the application of the GLCM and other analysis to images taken below the surface. Layers of z-stacked images analyzed as a group are another potential method for addressing the challenge of determining fluorescein permeability at depth. Moving from surface images that the current algorithm can accurately assess along z-stacks may allow for identification of confounding features which can then be worked around or addressed.

Utilizing z-stacked images may even prove to be a method to improve on the sensitivity and specificity of the current test.

The other major challenge of the method utilized in this study is the lack of an ordinal ranking system or a continuous scale that can be applied from the GLCM measures. This study is limited to a nominal system which determines simply whether the mucosa being imaged has an increased permeability or normal permeability. Future study will focus on adapting this current technique to an ordinal ranking system of multiple levels. An ordinal approach can then be compared to the more simplistic nominal approach to determine which system is best suited for clinical and research applications. Even with a working ordinal system, it may be advantageous to keep a more simplistic system in use for ease of clinical use. A future study will examine selecting multiple cut-off points to determine 3-5 distinct levels of permeability. These permeability levels may be compared against a visual grading system or compared to other quantitative means such as the Ussing chamber permeability measure or the lactulose/mannitol absorption method.

Retrospective analysis has examined previously obtained images to determine an ideal system for quantification of permeability. Future study will attempt to apply the system prospectively in conjunction with other permeability measures to further validate this approach. A focus will be placed on expanding the imaging region to include images obtained at increased depths such as in the lamina propria and on converting the current nominal rating scale to an ordinal measure. Prospective analysis will further develop this technique for eventual application in the clinic in real time diagnosis of gastrointestinal disease.

This study utilized fluorescein dye infusion during confocal endomicroscopy to obtain rectal epithelial images in an ovine model and analyzed these images using GLCM texture analysis. The correlation statistic from this approach was determined to be significantly different between untreated non-permeable images and images with an increased permeability due to BZK treatement. A cut-off value for the correlation statistic was obtained to examine a test set of images with a 95.5% sensitivity rating. Future prospective analysis utilizing a ranked scale for various permeability levels in conjunction with a comparison to another permeability measure will further develop and validate this approach for future clinical use.

Chapter 4 Comparison of confocal endomicroscopy permeability and microstructure at variable estrogen levels

SUMMARY

Gastrointestinal diseases such as irritable bowel syndrome have been demonstrated to occur at a higher rate in females. This phenomenon has been suggested to be due to the effects of estrogen in previous studies. Estrogen has been shown to strengthen tight junctions when present in a murine model. Confocal endomicroscopy is a newly emerging technique that can be combined with traditional endoscopy to provide information of epithelial permeability, structure, and the presence of inflammation. This study utilizes confocal endomicroscopy in a murine model at varying estrogen levels to assess the role of estrogen in functional membrane permeability and structural changes. Permeability is found to be increased in sheep with lower estrogen values, which is consistent with previous findings. The number of epithelial gaps due to cell shedding is additionally noted to potentially be higher in sheep with low estrogen values. These results indicate that estrogen has a protective effect on gut mucosa and results in decreased levels of inflammation and permeability.

INTRODUCTION

There are various disease states that have a significantly different gender distribution. In particular, autoimmune diseases often have an increased prevalence in females, with irritable bowel syndrome having a 4:1 predominance among women (15). Estrogen has been shown to alter gut permeability, with increased expression of tight junction proteins noted in rats when serum estrogen levels are high (20). This finding

suggests that it is paracellular permeability in particular that is modulated by systemic estrogen levels. Estrogen has additionally been noted to reduce permeability in rats using the Cr-labeled EDTA clearance method and the Ussing chamber method (20). Studies also show that blocking the effects of estradiol at the estrogen receptor β site reverses these alterations in permeability (19). Estrogen receptor β is found abundantly in the gut tissues. Each of these separate measures indicates that high serum estrogen levels produce a decrease in colonic permeability in a murine model. These findings can be correlated to clinical observations in observational studies of women with irritable bowel syndrome (57, 58). These studies demonstrate that IBS worsens in the days before menses. This corresponds to the diestrus phase of the hormonal cycle when estrogen levels are at their lowest. It is additionally found that a subset of female patients with IBS only have perimenstrual symptoms. In cycling females, the use of oral contraceptive agents has shown some success in treating a subset of patients with IBS (12, 14, 59). Despite these findings, post-menopausal women typically have decreased symptoms of IBS with lower levels of estrogen (12). In light of these apparent contradictions, the role of sex hormones in irritable bowel syndrome has not yet been fully characterized.

In addition to increased permeability to fluorescein, inflammatory conditions have been associated with other disruptions in the mucosal epithelial barrier, such as increased epithelial cell shedding. Intestinal epithelial cells are normally shed every 3 to 5 days as part of normal gut function (60). Microscopic imaging, such as by using confocal microscopy, of normal intestinal epithelium in a variety of species will show gaps in the epithelium that represent cells that have been shed. Inflammatory conditions such as IL-10 knockout mice cause an increase in cell shedding that can be quantified by counting

the number of cellular gaps per 1000 cells present (60). This work has been extended into the clinic in patients who have inflammatory bowel disease. Patients with IBD similarly have an increased number of cellular gaps per 1000 cells (60). Inflammation and disruption of the cellular epithelium is therefore associated with an increase in permeability via regulation of tight junctions, and also through an increase in epithelial cell shedding (10, 60). Small increases in the number of epithelial gaps may not significantly affect permeability, but in frank inflammatory states such as IBD, these gaps may contribute to changes in permeability. In summary, cell shedding and epithelial gaps noted on confocal images represent another method in addition to fluorescein leakage to assess disruption of the gut epithelium and underlying inflammation.

Confocal endomicroscopy imaging along with the systemic administration of fluorescein dye is an innovative method for assessing mucosal epithelial permeability. This technique has significant advantages over current methods in that it can assess functional permeability as well as structural integrity simultaneously in real time (6, 8). Additionally, this technique is minimally invasive when compared to techniques such as the Ussing chamber permeability measure. Confocal endomicroscopy can also be performed concurrently with endoscopic procedures, making it of particular interest for future clinical applications. It is already applied in upper endoscopic imaging to aid in the diagnosis of the metaplastic condition Barret's esophagus (6). Future applications may include helping to assess permeability in conditions such as leaky gut and irritable bowel syndrome, or in screening for neoplastic polyps during routine colonoscopy.

Permeability is assessed during CE by examining the quantity of fluorescein dye that leaks through the mucosal epithelium. Tight junctions, adherens junctions, and other

mechanisms normally keep this barrier relatively impermeable to fluorescein dye leaking from the interstitial tissue out into the gut lumen. However, when damage is induced by a variety of mechanisms, mucosal permeability can be increased as the barrier function is compromised (29, 44). Increased permeability is implicated in a variety of diseases and conditions, and is even suggested to increase susceptibility to contracting the HIV infection. A clinical visual grading scale exists to assess structural damage and functional permeability of these tissues (10, 38).

This study aims to assess fluorescein infusion and CE imaging assessment of the sigmorectal colon in an ovine model at varying estrogen levels. It is hypothesized that higher estrogen levels cause a decrease in permeability through the strengthening of tight junctions. Permeability as measured by the CE test is analyzed by the currently used visual grading system and by computer analysis. Other structural tissue observations are made such as lymphocyte distribution. In addition, cellular gaps per 1000 cells are examined as an additional measure of inflammation in the model.

MATERIALS AND METHODS

This study complies with all appropriate IACUC rules and regulations on animal experimentation and was reviewed by the board at UTMB before implementation. 4 Merino sheep weighing 35-45 kg were utilized in this study. They were kept on a strict 12-h light and 12-h dark cycle and fed twice daily, and were not fed on the morning of procedure days. Imaging was performed with an Optiscan FIVE1 laser scanning confocal endomicroscope. The rigid portion of the probe is 30 mm in length and the probe diameter is 5 mm. Light is provided by a 488 nm argon ion laser with collector set to 505-750 nm. Frame size is 475 x 475 µm and endoscopy is performed at 0.7 frames per

second. Resultant images are 1024 by 1024 pixels and are saved as TIFF files. Images may be obtained at depths of up to 70 μm. Image quality decreases at greater depths, so imaging is not typically performed at maximum depth. Throughout the procedure, different sites were assessed to provide diversity of test images.

Anesthesia for this procedure was 10 mg/kg of intramuscular ketamine, 10 mg/kg of intravenous ketamine, and 0.1 to 0.2 mg/kg of diazepam. Anesthesia was maintained during the procedure with 2-5% isoflurane gas. The sheep were positioned in the dorsal supine position throughout the procedure. Image contrast was provided by administering systemic fluorescein dye after baseline background images were obtained at the beginning of a new procedure. 25% fluorescein was injected as a bolus of 5 mL to begin the imaging procedure followed by an infusion rate of 1-3 mL/min throughout the remainder of the procedure. Fluorescein dye provides a measure of functional permeability and also provides contrast for sub-surface imaging into the lamina propria. After each imaging region was examined under fluorescein contrast, locally applied acriflavine dye was administered. 0.05% acriflavine in saline solution was administered directly into the rectal space and allowed to stain surface epithelium cells for sub-cellular contrast for 5 minutes before imaging was performed. Each imaging region was repeated after the acriflavine dye had been administered.

Imaging was performed at two different depths inside the rectum, with initial imaging performed 20 mm from the anus and the rest performed at 40 mm. In addition to surface images obtained at each site, images at depth were taken at several sites to evaluate the structure of the lamina propria and the visible vasculature. At each imaging site, an average of 5 images were taken to ensure quality images are obtained.

Lactulose and mannitol absorption testing was performed along with imaging to compare CE permeability assessment to a gold standard. After anesthesia was induced, a flexible gastroscope was passed down the esophagus and into the first stomach. 10 g of lactulose and 5 g of mannitol in 85 mL of sterile water was introduced through the scope and into the stomach. Serum was drawn at time points 0 hours, 1 hour, 3 hours, 6 hours, and 24 hours after introduction of the lactulose and mannitol solution. Analysis of lactulose and mannitol concentration in the serum was performed using the EnzyChrom Kits (BioAssay Systems EMNT-100 and ELTL-100).

The permeability of the rectal mucosa is altered by systemic estrogen levels. 2 sheep were treated with 100mg of depot medroxyprogesterone acetate (Depo-Provera) 4 weeks prior to imaging. Treatment with Depo-Provera causes an anestrous effect, with the levels of progesterone and estrogen being suppressed during the effect of the treatment. After 4 weeks, the hormone levels are fully suppressed and these two sheep could be said to be in anestrous. 2 other sheep were allowed to cycle naturally, and cycling was confirmed via ELISA testing for estradiol and progesterone (Abnova kits). Imaging on the cycling sheep was timed to fall early in the cycle, at a time of high estrogen levels. Estrous phase was further confirmed on the cycling sheep via trans-rectal ultrasound.

Images were analyzed in ImageJ (NIH Image) to quantitatively determine the number of permeable sites and to determine if there was an overall increase in permeability in each image set. The GLCM plug-in for ImageJ was run for each image to provide a correlation value, as was described in Chapter 3. The pixel step size was 1 and the angle 0 degrees. The percentage of sites that show increased permeability was

compared between the suppressed sheep and the normally cycling sheep using a Z test to compare two proportions with a p value of < 0.05 as significant. Qualitative observational methods were further recorded between the two groups for guidance of future study.

4 representative acriflavine stained images were chosen to perform a gaps per 1000 cells count on. 2 images were selected from the hormonally suppressed sheep group and 2 images were selected from the estrous phase cycling sheep, representing thousands of cells. Tiff format images were imported into ImageJ and cell counting was performed using the cell counter plug-in. Gaps were identified as dark areas in the epithelium around which cells could be visualized. Areas that were out of focus or in which cells were not visualized were not included in the count, and any dark spaces in these areas were not counted as gaps. The number of gaps per 1000 cells counted was calculated and compared between the two groups. Mean number of gaps per 1000 counted cells is computed along with standard deviation and difference is determined using the Student's t-test with a p value of <0.05 given as significant.

RESULTS

Representative confocal endomicroscopic images obtained from a suppressed sheep and a cycling estrous phase sheep are shown in Figure 4.1. Figure 4.1a shows a typical image from a site where increased permeability is noted. Instead of the marked increase in permeability that is easily observed in BZK treated images as in Chapter 2, the increase in permeability noted here is more subtle. The cellular definition seen on the surface of these images is usually easily seen, as in Figure 4.1b and in previously shown undamaged sites. However, Figure 4.1a shows a slight loss of cellular definition on the surface. In other, deeper images taken from the lamina propria in which the bottoms of the crypts are still visible show some pooling of dye in the suppressed sheep, which also

64

supports the finding of a slight increase in permeability. In Figure 4.1b, a typical estrus phase naturally cycling sheep image is seen, and no evidence of increased permeability is noted. Fluorescein may be seen in deeper slices of the image, but is limited to the capillaries and lamina propria, and did not leak into the lumen. Quantitative analysis utilizing the GLCM plugin and the produced correlation values as described in Chapter 3 yielded results for percentage of sites with increased permeability for both the suppressed and the cycling sheep. The suppressed sheep had 50% sites with increased permeability and the cycling sheep had 12.5% sites with increased permeability. The difference between these percentages is significant with a p value of <0.05. This was determined using the same ROC cut-off value that was calculated in Chapter 3 during previous analysis. The mean correlation value for suppressed sheep was 0.00111 (SD 0.000507) and the mean correlation value for cycling sheep was 0.00133 (SD 0.000567). These values are also significantly different, with the lower correlation value indicating a higher permeability in the suppressed, low hormone state sheep. Similar to the previous analysis performed on BZK treated sheep, the other GLCM computed values of angular second moment, contrast, inverse difference moment, and entropy did not significantly differ between groups.
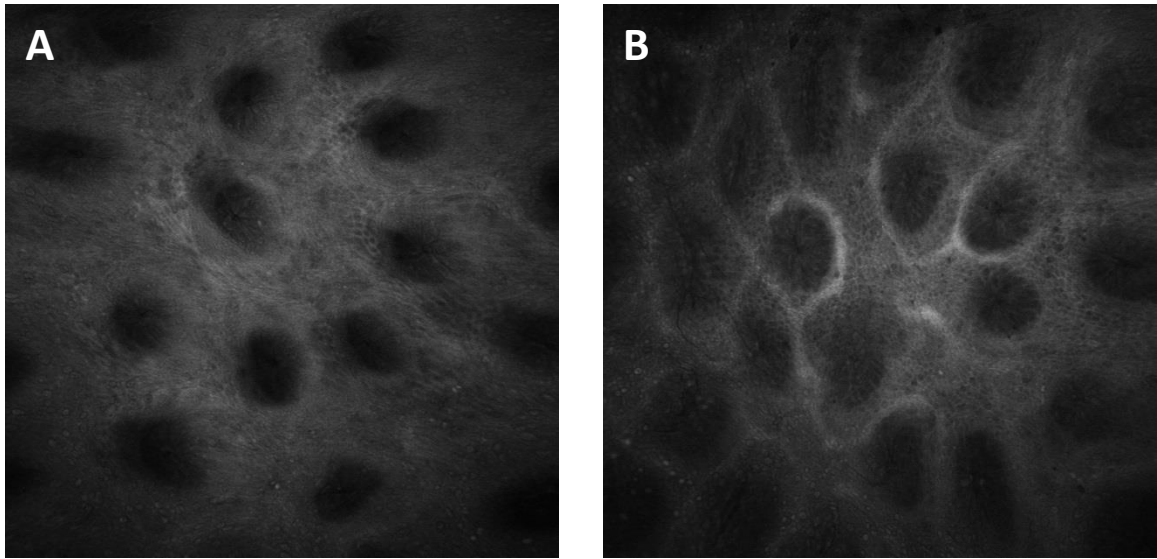
Figure 4.1:   Representative hormonally suppressed image and normal cycling image

In addition to the functional measures of barrier disruption indicated by an increase in permeability, the suppressed sheep show a subtle underlying inflammatory response. Images taken at depth in the lamina propria show a large number of extravasated leukocytes which are visible as dark cells that have gathered perivascularly in response to the decreased estrogen and progesterone state. Images in which these findings are noted are seen in Figure 4.2. Figure 4.2a shows a view of the lamina propria in a suppressed sheep where abundant leukocytes can be seen. The arrows in the image show several areas where leukocytes appear to be aggregating. Figure 4.2b shows a large lymphoid follicle of lymphocytes in the same sheep. Figure 4.2c includes a view of the capillary vasculature in the lamina propria of a hormonally suppressed sheep. The leukocytes can be seen throughout the image in the capillaries as well as immediately next to the capillaries as they extravasate. Figure 4.2d shows an image from an estrous phase cycling sheep in which leukocytes can be seen but in lesser numbers when compared to the suppressed images. The arrow in the image indicates an area where some leukocytes have gathered, but the numbers are significantly less than those seen gathered in Figure 4.2a or b.
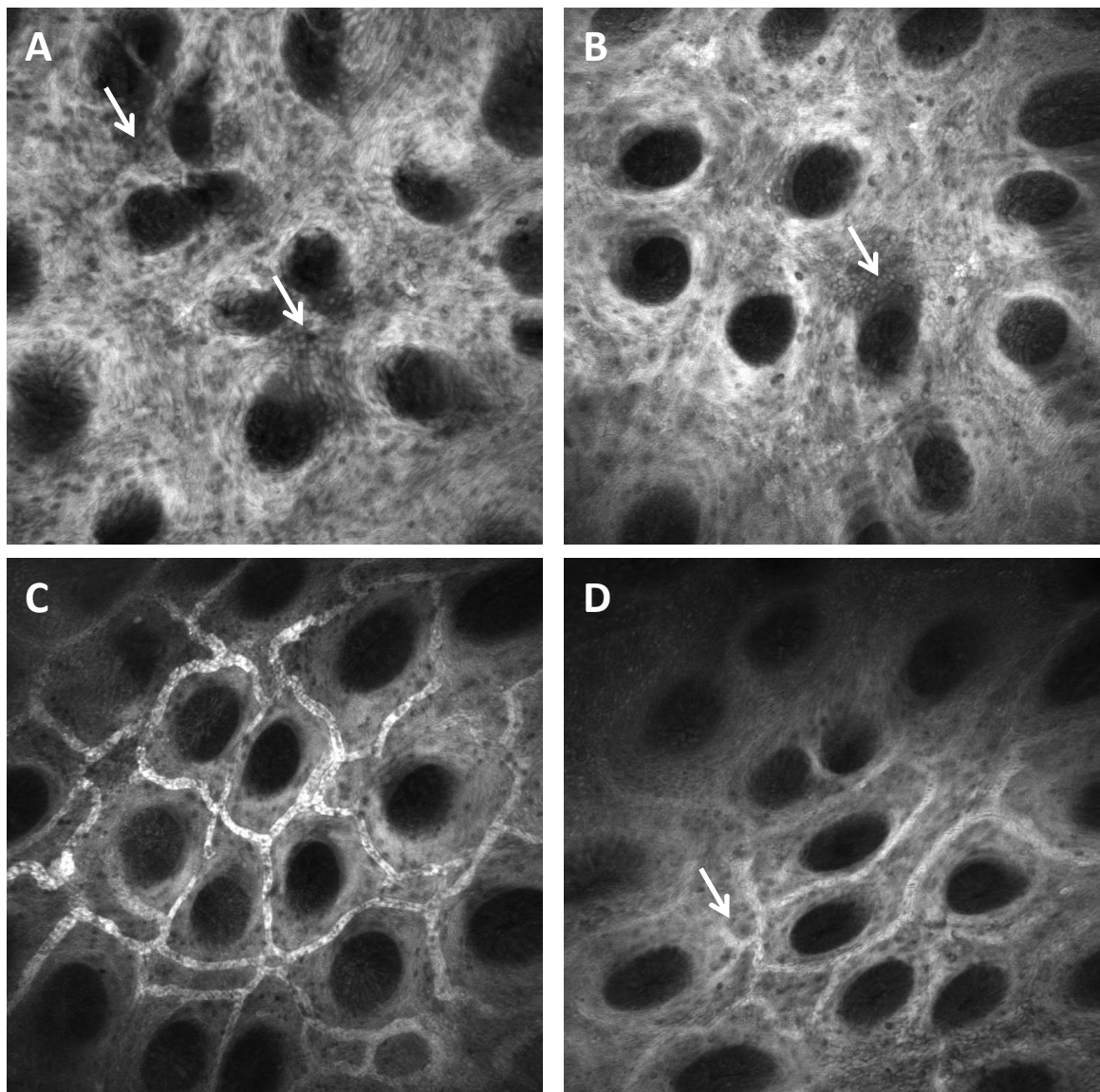
Figure 4.2:   Leukocytes aggregation seen in hormonally suppressed sheep (A-C) and in naturally cycling estrus phase sheep (D)

Epithelial gaps are normally found in colonic mucosa but an increased number of gaps is associated with inflammation and could cause an increase in permeability. Gaps may be noted in Figure 4.3. Figure 4.3a is an image from a hormonally suppressed sheep and Figure 4.3b is from the estrous phase normally cycling sheep. An epithelial gap is counted if a dark space is noted that is surrounded by epithelial cells, indicating a gap in

the epithelium. Dark areas that were more cellular in appearance are likely leukocytes and were not counted as gaps. There are some areas of leukocytes visible in Figure 4.3b, which can be contrasted with the gap indicated by the arrow. Utilizing the Cell Counter plugin in ImageJ (NIH Image) to manually count the gaps and epithelial cells, the number of epithelial gaps counted in the hormonally suppressed sheep was 10.8/1000 cells and the number of gaps counted in the estrous phase cycling sheep was 6.4/1000 cells. These results indicate that hormonally suppressed, low estrogen sheep may have more cell gaps in the epithelium, which is correlated with a corresponding increase in inflammation.
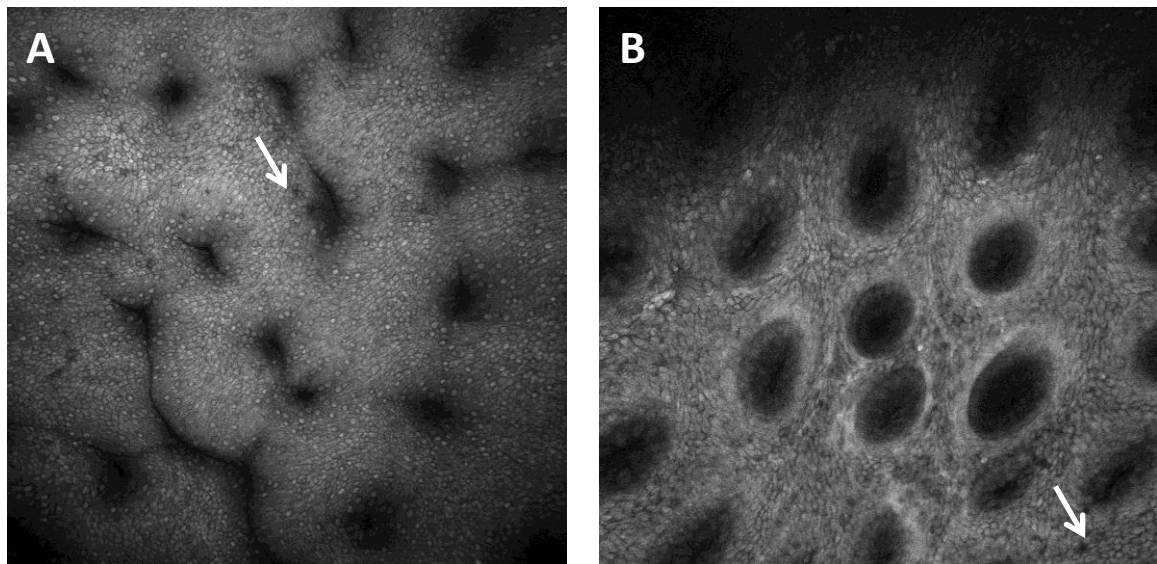
Figure 4.3:   Epithelial gaps noted due to cell shedding may be quantified

While CE imaging indicates an increase in permeability in hormonally suppressed sheep, preliminary lactulose/mannitol absorption testing did not detect changes, and may have been below the detection threshold of the kits that were used. In particular, mannitol testing revealed very little absorption of mannitol. The absorption of lactulose did produce an expected trend of increased serum lactulose up to a peak level at 6 hours of 9.6 μg/mL. However, the test did not produce a similar trend in all of the sheep tested.

Further testing with a revised protocol will be necessary to more definitively compare the CE permeability measure to the gold standard lactulose/mannitol assay.

DISCUSSION

Confocal endomicroscopy has gained clinical acceptance in the recent past and continues to be developed as a method for enhancing the ability of clinicians to better diagnose and treat a variety of conditions in real time. The ability for CE to assess both the functional status of epithelial tissues by measuring permeability and the structure of tissues by allowing for real time imaging make CE a unique tool. CE may have a role in the future in assisting in diagnosing and treating conditions such as irritable bowel syndrome and inflammatory bowel disease. However, CE is also used in translational studies to assess underlying pathophysiology behind clinical conditions. This study compared fluorescein dye infusion CE in an ovine model at varying estrogen level to determine the effects of estrogen on CE assessed permeability and microstructure. As has been shown previously, estrogen provides a protective effect to the intestinal epithelium and decreases permeability in a murine model as determined by other methods. CE confirms this finding as can be seen in Figure 4.1, where no increase in permeability is noted on estrous phase naturally cycling sheep images but a slight increase in permeability is noted on hormonally suppressed, low estrogen sheep. These results were confirmed quantitatively utilizing the algorithm developed in Chapter 3. These results confirm the feasibility of utilizing CE as a method for evaluating permeability and microstructure by confirming a previous finding in a new model. The increased permeability of the colonic epithelium at low estrogen levels corresponds to the reduced expression of tight junction proteins found previously (20). A decrease in permeability in

69

a high estrogen state in this study also correlates well with previous measures of reduced permeability via other methods in a murine model (20). In addition, CE provides other information beyond assessment of permeability.

The unique advantages of confocal endomicroscopy are further illustrated by the other data provided in a single imaging session. The ability to assess inflammation via the aggregation of leukocytes in the lamina propria of the colonic epithelium allows inflammation to be monitored that is otherwise invisible in white light imaging. The positions of these leukocytes as they move through the vasculature and extravasate into the lamina propria can be monitored in real time via CE. In this way, both acute and chronic inflammatory responses can be assessed. The number of leukocytes present may influence a number of factors in determining epithelial barrier integrity via the inflammatory cascade. Alterations in permeability, along with evidence of an increased inflammatory response have applications in a wide variety of diseases where early inflammation may predict further development of disease. Ulcerative colitis and Crohn's disease are excellent examples of this disease process. The ability for a clinician to evaluate inflammation via CE during endoscopy may allow for better treatment and prophylactic control of these diseases.

CE also provides additional structural information by allowing the number of epithelial gaps per area to be counted. While this metric is not available in real time during the procedure, it still provides an excellent indication of inflammation and a potential increase in permeability. Previous evidence has shown that inflammatory conditions cause a significant increase in the number of epithelial gaps per 1000 cells counted in the intestine. The results in this study are supportive of those findings and

indicate that Depo-Provera treatment to suppress the hormonal cycle in the sheep may cause an inflammatory response that increases the number of gaps that occur per 1000 cells. While this increase is not as significant as that noted in a disease such as inflammatory bowel disease, it still represents a significant inflammatory finding (57, 60).

The quantification of leukocytes as well as the identification of the type of leukocytes seen is an important topic for future study. A counting technique similar to that used for the epithelial gaps may be utilized to determine the number of leukocytes present per unit of area or per number of intestinal cells visible. Specifically, the identification of perivascular leukocytes and leukocytes that are actively extravasating may identify acute and active inflammation. This may be contrasted to aggregation of lymphoid follicles which may represent a more chronic inflammation. Biopsy specimens with staining or other methods for cell identification would assist in learning the type of leukocytes that are being observed. Identification of the types of cells may allow for better visual identification of the type of response noted. Along with better quantification of the leukocytes observed, it will be important to examine different test situations in which an increase in leukocytes may be observed. It would be of use to perform repeated BZK treatment or treatment with an alternative microbe to examine the response of tissue on a longer time course.

CE with fluorescein infusion represents a novel method for assessment of permeability, but has not been compared directly to other permeability measures. Lactulose/mannitol absorption with serum or urine collection allows for determination of permeability at various locations throughout the gut. The lactulose molecules are

absorbed paracellularly and the mannitol levels serve as a control as they are absorbed transcellurly. The lactulose to mannitol ratio is calculated to assess for alterations in permeability. An increase in this ratio would be noted when inflammation has occurred and paracellular permeability has been increased without a corresponding increase in transcellular mannitol permeability. The literature varies as to what qualifies as a normal lactulose/mannitol ratio, but the cutoff value is usually given as 0.05 to 0.07. Ratios below this value are considered to be normal and ratios above are considered to be abnormal. It may also be of value to examine the absolute lactulose and mannitol values that are present in serum at specific time points after administration. A revised protocol for a more complete comparison of CE assessment of permeability to a gold standard measurement such as the lactulose/mannitol absorption test may be of use in further validating CE as a permeability measure. Performing the test separately from imaging and increasing the doses of lactulose and mannitol that are administered may improve the results of this test.

Other topics of future study include the continuation of this current study to include luteal phase measurements on naturally cycling sheep as well as administration of added estrogen to the hormonally suppressed sheep to raise the estrogen level for comparison. This will allow for a wider variety of data for comparison to confirm the findings from this current study. Additionally, biopsy specimens can be acquired for histological analysis as well as immunohistochemistry staining for specific tight junction proteins implicated in alterations in permeability. This will allow this ovine model to be directly compared with similar previous studies in which expression of tight junction proteins was shown to be altered at varying estrogen level.

Confocal endomicroscopy is an emerging technology capable of combining real time subcellular level structural visualization with functional measures of permeability in the clinic during endoscopy procedure. The further development of this unique tool to adapt its use for the diagnosis and treatment of additional diseases represents an important step forward in the treatment of gastrointestinal diseases. This study provides interesting data and supports earlier studies that illustrate the influence of estrogen on gut permeability, as well as providing additional information on inflammatory features such as leukocyte aggregation and the presence of epithelial gaps. Further study is still required to continue to elicit the full role of estrogen on gastrointestinal diseases and chronic inflammatory states.

Chapter 5 Conclusions

Perturbations to the gastrointestinal mucosal surface epithelium have been associated with a number of disease states. The exposure of submucosal surfaces to normal gut flora as well as any material, toxins, or pathogens that may be in the intestinal lumen may be detrimental to the underlying tissue and cause infection or inflammation. Maintenance of the intestinal barrier is important in preventing a number of diseases. The assessment of barrier function has traditionally been performed via endoscopy and white light imaging or by histological assessment of biopsy specimens by a pathologist. Confocal endomicroscopy is an emerging method for augmenting and expanding the current capabilities of traditional endoscopy. CE is capable of assessing functional measures such as permeability while also providing subcellular resolution images of structural features in tissue. In addition, CE provides images below the mucosal surface without the need for a biopsy. CE is currently utilized clinically in several ways such as assessment of metaplasia in the esophagus and guidance of biopsy in potential cases of colorectal cancer. However, there are many further applications for CE.

Chapter 2 examines the use of CE as a method to evaluate topical drug agents such as the microbicidal gel BZK. BZK is demonstrated to increase the permeability and destroy the structural integrity of the rectal mucosal barrier. As BZK is employed as a microbicidal gel, this finding has implications in transmission of sexually transmitted diseases such as HIV. Loss of the mucosal barrier in the rectum can increase the susceptibility to infection. Chapter 2 demonstrates that CE is a practical method to assess agents such as BZK in an *in vivo* ovine model that may be expanded to other similar applications.

While CE has been used previously in conjunction with a qualitative grading system to assess permeability, Chapter 3 expands on this concept and introduces an algorithm that is capable of quantitatively determining whether a test image is permeable

or not. The quantification of CE permeability measures expands its potential uses. Real time quantitative permeability measures during endoscopy without the need for biopsy or other tests may be possible utilizing a similar method. While further work is needed to expand the algorithm method to a permeability ranking system, this method lays the foundation for quantitative permeability assessment using confocal methods.

Chapter 4 applies the method developed in Chapter 3 to an interesting clinical correlation between estrogen level and GI diseases such as irritable bowel syndrome. IBS has a strong female predominance. Chapter 4 applies CE to an ovine variable estrogen level model to assess the changes in permeability and structure in the gut. An increase in permeability is noted in sheep who have suppressed hormone levels, while no increase is noted in estrous phase normally cycling sheep. These results confirm previous results from murine studies that indicate estrogen strengthens tight junctions and lowers permeability. CE may be a future method to help diagnose IBS, as there is currently no empirical test available for it. In addition, this study helps confirm the findings in Chapter 3 and tests the quantitative permeability method. Future study will expand on these findings and will work to correlate confocal findings in this ovine model with other accepted measures of permeability such as the lactulose/mannitol absorption test. This will further validate CE as a reliable measure of permeability that is more easily implemented than alternative methods.

Confocal endomicroscopy was used to assess rectal susceptibility to HIV and to assess the role of estrogen in gastrointestinal diseases. A quantitative method was developed for permeability measurement using the CE plus fluorescein infusion method. These studies expand on the potential uses for CE in the clinical and laboratory setting in the future and provide many avenues for expanded future work.

References

1.   Kiesslich R, Burg J, Vieth M, Gnaendiger J, Enders M, Delaney P, et al. Confocal laser endoscopy for diagnosing intraepithelial neoplasias and colorectal cancer in vivo. Gastroenterology. 2004;127(3):706-13. PubMed PMID: 15362025.

2.   Hurlstone DP, Tiffin N, Brown SR, Baraza W, Thomson M, Cross SS. In vivo confocal laser scanning chromo-endomicroscopy of colorectal neoplasia: changing the technological paradigm. Histopathology. 2008;52(4):417-26. doi: 10.1111/j.1365-2559.2007.02842.x. PubMed PMID: 17903203.

3.   Goetz M, Kiesslich R. Confocal endomicroscopy: in vivo diagnosis of neoplastic lesions of the gastrointestinal tract. Anticancer Res. 2008;28(1B):353-60. PubMed PMID: 18383869.

4.   Smith LA, Tiffin N, Thomson M, Cross SS, Hurlstone DP. Chromoscopic endomicroscopy: in vivo cellular resolution imaging of the colorectum. J Gastroenterol Hepatol. 2008;23(7 Pt 1):1009-23. doi: 10.1111/j.1440-1746.2008.05463.x. PubMed PMID: 18557799.

5.   Paull PE, Hyatt BJ, Wassef W, Fischer AH. Confocal laser endomicroscopy: a primer for pathologists. Arch Pathol Lab Med. 2011;135(10):1343-8. doi: 10.5858/arpa.2010-0264-RA. PubMed PMID: 21970490.

6.   Committee AT. Confocal laser endomicroscopy. Gastrointest Endosc. 2014;80(6):928-38. doi: 10.1016/j.gie.2014.06.021. PubMed PMID: 25442092.

7.   Kiesslich R, Galle PR, Neurath M. Atlas of endomicroscopy. Heidelberg: Springer; 2008. xiv, 103 p. p.

8.   Goetz M, Watson A, Kiesslich R. Confocal laser endomicroscopy in gastrointestinal diseases. J Biophotonics. 2011;4(7-8):498-508. doi: 10.1002/jbio.201100022. PubMed PMID: 21567975.

9.   Kamen A, Sun S, Wan S, Kluckner S, Chen T, Gigler AM, et al. Automatic Tissue Differentiation Based on Confocal Endomicroscopic Images for Intraoperative Guidance in Neurosurgery. Biomed Res Int. 2016;2016:6183218. doi: 10.1155/2016/6183218. PubMed PMID: 27127791; PubMed Central PMCID: PMCPMC4835625.

10.   Kiesslich R, Duckworth CA, Moussata D, Gloeckner A, Lim LG, Goetz M, et al. Local barrier dysfunction identified by confocal laser endomicroscopy predicts relapse in inflammatory bowel disease. Gut. 2012;61(8):1146-53. doi: 10.1136/gutjnl-2011-300695. PubMed PMID: 22115910; PubMed Central PMCID: PMCPMC3388727.

11.   Moussata D, Goetz M, Gloeckner A, Kerner M, Campbell B, Hoffman A, et al. Confocal laser endomicroscopy is a new imaging modality for recognition of intramucosal bacteria in inflammatory bowel disease in vivo. Gut. 2011;60(1):26-33. doi: 10.1136/gut.2010.213264. PubMed PMID: 20980342; PubMed Central PMCID: PMCPMC3002833.

12.   Mulak A, Taché Y, Larauche M. Sex hormones in the modulation of irritable bowel syndrome. World J Gastroenterol. 2014;20(10):2433-48. doi: 10.3748/wjg.v20.i10.2433. PubMed PMID: 24627581; PubMed Central PMCID: PMCPMC3949254.

13.   Houghton LA, Jackson NA, Whorwell PJ, Morris J. Do male sex hormones protect from irritable bowel syndrome? Am J Gastroenterol. 2000;95(9):2296-300. doi: 10.1111/j.1572-0241.2000.02314.x. PubMed PMID: 11007231.

14.   Matricon J, Meleine M, Gelot A, Piche T, Dapoigny M, Muller E, et al. Review article: Associations between immune activation, intestinal permeability and the irritable bowel syndrome. Aliment Pharmacol Ther. 2012;36(11-12):1009-31. doi: 10.1111/apt.12080. PubMed PMID: 23066886.

15.   Meleine M, Matricon J. Gender-related differences in irritable bowel syndrome: potential mechanisms of sex hormones. World J Gastroenterol. 2014;20(22):6725-43. doi: 10.3748/wjg.v20.i22.6725. PubMed PMID: 24944465; PubMed Central PMCID: PMCPMC4051914.

16.   Piche T, Barbara G, Aubert P, Bruley des Varannes S, Dainese R, Nano JL, et al. Impaired intestinal barrier integrity in the colon of patients with irritable bowel syndrome: involvement of soluble mediators. Gut. 2009;58(2):196-201. doi: 10.1136/gut.2007.140806. PubMed PMID: 18824556.

17.   Zhou Q, Zhang B, Verne GN. Intestinal membrane permeability and hypersensitivity in the irritable bowel syndrome. Pain. 2009;146(1-2):41-6. doi: 10.1016/j.pain.2009.06.017. PubMed PMID: 19595511; PubMed Central PMCID: PMCPMC2763174.

18.   Minuti A, Ahmed S, Trevisi E, Piccioli-Cappelli F, Bertoni G, Bani P. Assessment of gastrointestinal permeability by lactulose test in sheep after repeated indomethacin treatment. J Anim Sci. 2013;91(12):5646-53. doi: 10.2527/jas.2013-6729. PubMed PMID: 24126268.

19.   Looijer-van Langen M, Hotte N, Dieleman LA, Albert E, Mulder C, Madsen KL. Estrogen receptor-β signaling modulates epithelial barrier function. Am J Physiol Gastrointest Liver Physiol. 2011;300(4):G621-6. doi: 10.1152/ajpgi.00274.2010. PubMed PMID: 21252046.

20.   Braniste V, Leveque M, Buisson-Brenac C, Bueno L, Fioramonti J, Houdeau E. Oestradiol decreases colonic permeability through oestrogen receptor beta-mediated up-regulation of occludin and junctional adhesion molecule-A in epithelial cells. J Physiol. 2009;587(Pt 13):3317-28. doi: 10.1113/jphysiol.2009.169300. PubMed PMID: 19433574; PubMed Central PMCID: PMCPMC2727039.

21.   Braniste V, Jouault A, Gaultier E, Polizzi A, Buisson-Brenac C, Leveque M, et al. Impact of oral bisphenol A at reference doses on intestinal barrier function and sex differences after perinatal exposure in rats. Proc Natl Acad Sci U S A. 2010;107(1):448-53. doi: 10.1073/pnas.0907697107. PubMed PMID: 20018722; PubMed Central PMCID: PMCPMC2806743.

22.   Moussa L, Bézirard V, Salvador-Cartier C, Bacquié V, Houdeau E, Théodorou V. A new soy germ fermented ingredient displays estrogenic and protease inhibitor activities able to prevent irritable bowel syndrome-like symptoms in stressed female rats. Clin Nutr. 2013;32(1):51-8. doi: 10.1016/j.clnu.2012.05.021. PubMed PMID: 22727545.

23.   Triadafilopoulos G, Finlayson M, Grellet C. Bowel dysfunction in postmenopausal women. Women Health. 1998;27(4):55-66. doi: 10.1300/J013v27n04_04. PubMed PMID: 9796084.

24.   CDC. Diagnoses of HIV Infection in the United States and Dependent Areas. HIV Surveillance Report; 2014.

25.   Prejean J, Song R, Hernandez A, Ziebell R, Green T, Walker F, et al. Estimated HIV incidence in the United States, 2006-2009. PLoS One. 2011;6(8):e17502. doi: 10.1371/journal.pone.0017502. PubMed PMID: 21826193; PubMed Central PMCID: PMCPMC3149556.

26.   Peterson LW, Artis D. Intestinal epithelial cells: regulators of barrier function and immune homeostasis. Nat Rev Immunol. 2014;14(3):141-53. doi: 10.1038/nri3608. PubMed PMID: 24566914.

27.   McElrath MJ, Smythe K, Randolph-Habecker J, Melton KR, Goodpaster TA, Hughes SM, et al. Comprehensive assessment of HIV target cells in the distal human gut suggests increasing HIV susceptibility toward the anus. J Acquir Immune Defic Syndr. 2013;63(3):263-71. doi: 10.1097/QAI.0b013e3182898392. PubMed PMID: 23392465; PubMed Central PMCID: PMCPMC3683090.

28.   Baggaley RF, Dimitrov D, Owen BN, Pickles M, Butler AR, Masse B, et al. Heterosexual anal intercourse: a neglected risk factor for HIV? Am J Reprod Immunol. 2013;69 Suppl 1:95-105. doi: 10.1111/aji.12064. PubMed PMID: 23279040; PubMed Central PMCID: PMCPMC3938911.

29.   Burgener A, McGowan I, Klatt NR. HIV and mucosal barrier interactions: consequences for transmission and pathogenesis. Curr Opin Immunol. 2015;36:22-30. doi: 10.1016/j.coi.2015.06.004. PubMed PMID: 26151777.

30.   Mesquita PM, Cheshenko N, Wilson SS, Mhatre M, Guzman E, Fakioglu E, et al. Disruption of tight junctions by cellulose sulfate facilitates HIV infection: model of microbicide safety. J Infect Dis. 2009;200(4):599-608. doi: 10.1086/600867. PubMed PMID: 19586414; PubMed Central PMCID: PMCPMC2877491.

31.   Canary LA, Vinton CL, Morcock DR, Pierce JB, Estes JD, Brenchley JM, et al. Rate of AIDS progression is associated with gastrointestinal dysfunction in simian immunodeficiency virus-infected pigtail macaques. J Immunol. 2013;190(6):2959-65. doi: 10.4049/jimmunol.1202319. PubMed PMID: 23401593; PubMed Central PMCID: PMCPMC3665608.

32.   Fuchs EJ, Lee LA, Torbenson MS, Parsons TL, Bakshi RP, Guidos AM, et al. Hyperosmolar sexual lubricant causes epithelial damage in the distal colon: potential implication for HIV transmission. J Infect Dis. 2007;195(5):703-10. doi: 10.1086/511279. PubMed PMID: 17262713.

33.   Gorbach PM, Weiss RE, Fuchs E, Jeffries RA, Hezerah M, Brown S, et al. The slippery slope: lubricant use and rectal sexually transmitted infections: a newly identified risk. Sex Transm Dis. 2012;39(1):59-64. doi: 10.1097/OLQ.0b013e318235502b. PubMed PMID: 22183849; PubMed Central PMCID: PMCPMC3244680.

34.   Patton DL, Cosgrove Sweeney YT, Rabe LK, Hillier SL. Rectal applications of nonoxynol-9 cause tissue disruption in a monkey model. Sex Transm Dis. 2002;29(10):581-7. PubMed PMID: 12370525.

35.   Rebe KB, De Swardt G, Berman PA, Struthers H, McIntyre JA. Sexual lubricants in South Africa may potentially disrupt mucosal surfaces and increase HIV transmission risk among men who have sex with men. S Afr Med J. 2014;104(1):49-51. PubMed PMID: 24388089.

36.   Phillips DM, Sudol KM, Taylor CL, Guichard L, Elsen R, Maguire RA. Lubricants containing N-9 may enhance rectal transmission of HIV and other STIs. Contraception. 2004;70(2):107-10. doi: 10.1016/j.contraception.2004.04.008. PubMed PMID: 15288213.

37.   Fuchs EJ, Grohskopf LA, Lee LA, Bakshi RP, Hendrix CW. Quantitative assessment of altered rectal mucosal permeability due to rectally applied nonoxynol-9, biopsy, and simulated intercourse. J Infect Dis. 2013;207(9):1389-96. doi: 10.1093/infdis/jit030. PubMed PMID: 23325915; PubMed Central PMCID: PMCPMC3693591.

38.   Vargas G, Vincent KL, Zhu Y, Szafron D, Brown TC, Villareal PP, et al. In vivo rectal mucosal barrier function imaging in a large animal model using confocal endomicroscopy: implications for injury assessment and use in HIV prevention studies. Antimicrob Agents Chemother. 2016. doi: 10.1128/AAC.00134-16. PubMed PMID: 27185807.

39.   Mishra A, Makharia GK. Techniques of functional and motility test: how to perform and interpret intestinal permeability. J Neurogastroenterol Motil. 2012;18(4):443-7. doi: 10.5056/jnm.2012.18.4.443. PubMed PMID: 23106006; PubMed Central PMCID: PMCPMC3479259.

40.   Barbara G, De Giorgio R, Stanghellini V, Cremon C, Corinaldesi R. A role for inflammation in irritable bowel syndrome? Gut. 2002;51 Suppl 1:i41-4. PubMed PMID: 12077063; PubMed Central PMCID: PMCPMC1867730.

41.   Cremon C, Gargano L, Morselli-Labate AM, Santini D, Cogliandro RF, De Giorgio R, et al. Mucosal immune activation in irritable bowel syndrome: gender-dependence and association with digestive symptoms. Am J Gastroenterol. 2009;104(2):392-400. doi: 10.1038/ajg.2008.94. PubMed PMID: 19174797.

42.   Gué M, Del Rio-Lacheze C, Eutamene H, Théodorou V, Fioramonti J, Buéno L. Stress-induced visceral hypersensitivity to rectal distension in rats: role of CRF and mast cells. Neurogastroenterol Motil. 1997;9(4):271-9. PubMed PMID: 9430796.

43.   Barbara G, Stanghellini V, De Giorgio R, Corinaldesi R. Functional gastrointestinal disorders and mast cells: implications for therapy. Neurogastroenterol Motil. 2006;18(1):6-17. doi: 10.1111/j.1365-2982.2005.00685.x. PubMed PMID: 16371078.

44.   Artis D. Epithelial-cell recognition of commensal bacteria and maintenance of immune homeostasis in the gut. Nat Rev Immunol. 2008;8(6):411-20. doi: 10.1038/nri2316. PubMed PMID: 18469830.

45.   Hansson GC. Role of mucus layers in gut infection and inflammation. Curr Opin Microbiol. 2012;15(1):57-62. doi: 10.1016/j.mib.2011.11.002. PubMed PMID: 22177113; PubMed Central PMCID: PMCPMC3716454.

46.   Dezzutti CS, James VN, Ramos A, Sullivan ST, Siddig A, Bush TJ, et al. In vitro comparison of topical microbicides for prevention of human immunodeficiency virus type 1 transmission. Antimicrob Agents Chemother. 2004;48(10):3834-44. doi: 10.1128/AAC.48.10.3834-3844.2004. PubMed PMID: 15388443; PubMed Central PMCID: PMCPMC521884.

47.   Patton DL, Sweeney YT, Paul KJ. A summary of preclinical topical microbicide rectal safety and efficacy evaluations in a pigtailed macaque model. Sex Transm Dis. 2009;36(6):350-6. doi: 10.1097/OLQ.0b013e318195c31a. PubMed PMID: 19556929; PubMed Central PMCID: PMCPMC2749653.

48.   Abner SR, Guenthner PC, Guarner J, Hancock KA, Cummins JE, Fink A, et al. A human colorectal explant culture to evaluate topical microbicides for the prevention of HIV infection. J Infect Dis. 2005;192(9):1545-56. doi: 10.1086/462424. PubMed PMID: 16206069.

49.   Li W, Huang Z, Wu Y, Wang H, Zhou X, Xiao Z, et al. Effectiveness of an optimized benzalkonium chloride gel as vaginal contraceptive: a randomized controlled trial among Chinese women. Contraception. 2013;87(6):756-65. doi: 10.1016/j.contraception.2012.09.012. PubMed PMID: 23089047.

50.   Vincent KL, Vargas G, Bourne N, Galvan-Turner V, Saada JI, Lee GH, et al. Image-based noninvasive evaluation of colorectal mucosal injury in sheep after topical application of microbicides. Sex Transm Dis. 2013;40(11):854-9. doi:

10.1097/OLQ.0000000000000039. PubMed PMID: 24113407; PubMed Central PMCID: PMCPMC3901848.

51.   Vargas G, Patrikeev I, Wei J, Bell B, Vincent K, Bourne N, et al. Quantitative assessment of microbicide-induced injury in the ovine vaginal epithelium using confocal microendoscopy. BMC Infect Dis. 2012;12:48. doi: 10.1186/1471-2334-12-48. PubMed PMID: 22375797; PubMed Central PMCID: PMCPMC3315435.

52.   Vincent KL, Bell BA, Johnston RK, Stegall R, Vargas G, Tan A, et al. Benzalkonium chloride causes colposcopic changes and increased susceptibility to genital herpes infection in mice. Sex Transm Dis. 2010;37(9):579-84. PubMed PMID: 20803781.

53.   Marques PE, Antunes MM, David BA, Pereira RV, Teixeira MM, Menezes GB. Imaging liver biology in vivo using conventional confocal microscopy. Nat Protoc. 2015;10(2):258-68. doi: 10.1038/nprot.2015.006. PubMed PMID: 25569332.

54.   Zane A, McCracken C, Knight DA, Young T, Lutton AD, Olesik JW, et al. Uptake of bright fluorophore core-silica shell nanoparticles by biological systems. Int J Nanomedicine. 2015;10:1547-67. doi: 10.2147/IJN.S76208. PubMed PMID: 25759579; PubMed Central PMCID: PMCPMC4345991.

55.   Sheikhzadeh F, Ward RK, Carraro A, Chen ZY, van Niekerk D, Miller D, et al. Quantification of confocal fluorescence microscopy for the detection of cervical intraepithelial neoplasia. Biomed Eng Online. 2015;14:96. doi: 10.1186/s12938-015-0093-6. PubMed PMID: 26499452; PubMed Central PMCID: PMCPMC4619300.

56.   Haralick R, Shanmugam K, Dinstein Ih. Textural Features for Image Classification. IEEE Transactions of Systems, Man and Cybernetics; 1973. p. 610-21.

57.   Straub RH. The complex role of estrogens in inflammation. Endocr Rev. 2007;28(5):521-74. doi: 10.1210/er.2007-0001. PubMed PMID: 17640948.

58.   Wada-Hiraike O, Imamov O, Hiraike H, Hultenby K, Schwend T, Omoto Y, et al. Role of estrogen receptor beta in colonic epithelium. Proc Natl Acad Sci U S A. 2006;103(8):2959-64. doi: 10.1073/pnas.0511271103. PubMed PMID: 16477031; PubMed Central PMCID: PMCPMC1413854.

59.   Alonso C, Guilarte M, Vicario M, Ramos L, Rezzi S, Martínez C, et al. Acute experimental stress evokes a differential gender-determined increase in human intestinal

macromolecular permeability. Neurogastroenterol Motil. 2012;24(8):740-6, e348-9. doi: 10.1111/j.1365-2982.2012.01928.x. PubMed PMID: 22625665.

60.   Liu JJ, Madsen KL, Boulanger P, Dieleman LA, Meddings J, Fedorak RN. Mind the gaps: confocal endomicroscopy showed increased density of small bowel epithelial gaps in inflammatory bowel disease. J Clin Gastroenterol. 2011;45(3):240-5. doi: 10.1097/MCG.0b013e3181fbdb8a. PubMed PMID: 21030873.

Author Vita

David Szafron was born on October 9, 1989 in Chicago, IL to Kevin and Marie Szafron. David moved to Houston, Texas at the age of 5 and attended school in the Clear Lake area. David graduated from Clear Lake High School in 2008 and then completed his undergraduate degree at Texas A&M University in College Station, TX. He received a Bachelor's of Science in Biomedical Engineering and graduated in 2012. During his undergraduate years, he worked in Dr. Duncan Maitland's lab and was a co-author on a publication published in 2013. He entered medical school at the University of Texas Medical Branch in Galveston, Texas in 2012 and additionally completed a Masters of Clinical Science degree during a research year between his 3rd and 4th years of medical school. David will graduate from medical school in 2017 and enter a residency program in Internal Medicine.

Permanent address: 25503 Greenwell Springs Lane, Katy, TX, 77494

This thesis was typed by David Szafron.